

SANCScope – v.1.00

A. Andonov, A. Arbuzov*, D. Bardin, S. Bondarenko*,
P. Christova, L. Kalinovskaya, G. Nanava**, and W. von Schlippe***

*Dzhelepov Laboratory for Nuclear Problems, JINR,
* Bogoliubov Laboratory of Theoretical Physics, JINR,
ul. Joliot-Curie 6, RU-141980 Dubna, Russia,
** on leave from IHEP, TSU, Tbilisi, Georgia,
*** Petersburg Nuclear Physics Institute,
Gatchina, RU-188300 St. Petersburg, Russia*

Abstract

In this article we have summarized the status of the system **SANC** version 1.00. We have implemented theoretical predictions for many high energy interactions of fundamental particles at the one-loop precision level for up to 4-particle processes. In the present part of our **SANC** description we place emphasis on an extensive discussion of an important first step of calculations of the one-loop amplitudes of 3- and 4-particle processes in QED, QCD and EW theories.

SANC version v1.00 is accessible from servers at Dubna <http://sanc.jinr.ru/> (159.93.74.10) and CERN <http://pcphsanc.cern.ch/> (137.138.180.42).

(To be published in Computer Physics Communications)

Contents

1	Introduction	4
2	Amplitude Basis, Scalar Form Factors, Helicity Amplitudes	6
2.1	Introduction	6
2.2	The 3-leg processes $B(Q) \rightarrow f(p_1) + \bar{f}(p_2)$	6
2.3	The 3-leg processes $B(Q) \rightarrow V(p_1) + V(p_2)$, $V = \gamma, Z, W$	9
2.4	The 4-leg NC processes $f_1 \bar{f}_1 \rightarrow (\gamma Z) \rightarrow f \bar{f}$	10
2.5	The 4-leg CC processes $f_1 \bar{f}'_1 \rightarrow (W) \rightarrow f \bar{f}'$	12
2.6	Bhabha scattering	14
2.7	$f f b b \rightarrow 0$ processes	15
3	Precomputation	17
3.1	Introduction	17
3.2	Self energies	19
3.2.1	Bosonic self energy	19
3.2.2	Fermionic self energy	21
3.2.3	Fermionic self energy for $f f b b$ processes	23
3.3	One-loop vertices	24
3.3.1	$b f \bar{f}$ vertices	24
3.3.2	$b b b$ vertices	25
3.3.3	Vertices for $f f b b$ processes	26
3.4	One-loop boxes	28
3.4.1	Boxes for $f f f f$ processes	28
3.4.2	Boxes for $f f b b$ processes	29
4	SANC Procedures	34
4.1	Introduction	34
4.2	Intrinsic procedures	34
4.3	Feynman rules	39
5	Processes, available in SANC v.1.00	41
6	User Guide	43
6.1	Getting started	43
6.1.1	SANC installation	43
6.1.2	SANC windows	43
6.1.3	Login procedure	43
6.1.4	The SANC tree	43
6.1.5	Naming conventions	44
6.2	Benchmark case 1: $b \rightarrow f f$ decays	46
6.2.1	Semianalytical calculation	46
6.2.2	Monte Carlo calculation	47
6.3	Benchmark case 2: the process $2f \rightarrow 2f$	47
	Acknowledgments	48
	References	49

List of Figures

1	$f_1 \bar{f}_1 \rightarrow f \bar{f}$ process	10
2	Precomputation in QED part	17
3	Precomputation in EW part	18
4	Bosonic self energy, two point diagrams	19
5	Bosonic self energy, one point diagrams	19
6	Bosonic self energy, tadpoles	19
7	Fermionic self energy, two point diagrams	21
8	Fermionic self energy, tadpoles	22
9	Self energy $f f b b$ diagrams	23
10	$b f f$ vertices	24
11	$b b b$ vertices	25
12	$f f b b$ vertices	27
13	$f f f f$ boxes, direct and crossed	28
14	$f f b b$ boxes, topologies T2 and T4	30
15	$f f b b$ boxes, topologies T1 and T3	31
16	$f f b b$ boxes, topologies T5 and T6	32
17	$f f b b$ boxes, topology T7	33
18	Available processes in QED part	41
19	Available processes in EW part	42
20	Main SANC window	45

List of Tables

1	The SANC Menus and their options.	44
2	List of fields.	44
3	Benchmark Results for $\Gamma(Z \rightarrow b \bar{b})$ decay	47
4	Assignment of particle numbers for process $u \bar{d} \rightarrow e^+ \nu_e$	47
5	CMS differential cross sections in pb for $u \bar{d} \rightarrow e^+ \nu_e$	48

PROGRAM SUMMARY

- *Title of program:* SANC
- *Catalogue identifier:*
- *Program obtainable from:* Internet sites at DLNP, JINR, Dubna, Russia, <http://sanc.jinr.ru/> (159.93.74.10) and at CERN, <http://pcphsanc.cern.ch> (137.138.180.42)
- *Computers for which the program is designed and others on which it has been tested:*
Designed for: platforms on which Java and FORM3 are available
Tested on: Intel-based PC's
- *Operating systems:* Linux, Windows
- *Programming languages used:* Java, FORM3, PERL, FORTRAN
- *Memory required to execute with typical data:* 10 Mb
- *No. of bits in a word:* 32
- *No. of processors used:* 1 on SANC server, 1 on SANC client
- *Distribution format:* gzipped tar archive
- *Keywords:* Feynman diagrams, Perturbation theory, Quantum field theory, Standard Model, Electroweak interactions, QCD, QED, One-loop calculations, Monte Carlo generators.
- *Nature of physical problem:* Automatic calculation of pseudo- and realistic observables for various processes and decays in the Standard Model of Electroweak interactions, QCD and QED at one-loop precision level. Form factors and helicity amplitudes free of UV divergences are produced. For exclusion of IR singularities the soft photon emission is included.
- *Method of Solution:* Numerical computation of analytical formulae of form factors and helicity amplitudes. For simulation of two fermion radiative decays of Standard Model bosons (W^\pm, Z) and the Higgs boson a Monte Carlo technique is used.
- *Restrictions on the complexity:* In the current version of SANC there are 3 and 4 particle processes and decays available at one-loop precision level.
- *Typical Running time:* The running time depends on the selected process. For instance, the symbolic calculation of form factors (with precomputed building blocks) of Bhabha scattering in the Standard Model takes about 15 sec, helicity amplitudes — about 30 sec, and bremsstrahlung — 10 sec. The numerical computation of cross-section for this process takes about 5 sec (CPU 3GHz IP4, RAM 512Mb, L2 1024 KB).

1 Introduction

Project motivation

The main goal is the creation of a computer system for semi-automatic calculations of realistic and pseudo-observables for various processes of elementary particle interactions “from the SM Lagrangian to event distributions” at the one-loop precision level for the present and future colliders – TEVATRON (Runs II and III), LHC, electron Linear Colliders (ISCLC, CLIC), muon factories and others.

Furthermore, the **SANC** system, even at the level which is reached already, may be used for educational purposes by students specializing in high energy physics. With its help, it is easy to follow all steps of calculations at the one-loop precision level for $W, Z, H \rightarrow f\bar{f}(\gamma)$, $H \rightarrow \gamma\gamma, Z\gamma, ZZ, WW$, $t \rightarrow bW$ decays, and many other processes. Moreover, all the calculations are realized in the spirit of the book [1] which makes the **SANC** system particularly appealing for pedagogical purposes.

Historical overview

The **SANC** project has been started in early 2001. During the first phase of the project (2001–2003), the **SANC** group demonstrated the workability of the computer system which is being developed [2]. The **version 0.01**, from 03/28/2001, was already able to compute one-loop Feynman diagrams for all SM $1 \rightarrow 2$ decays and $2f \rightarrow 2f$ processes (in R_ξ and unitary gauges, including QCD, accessing thereby all one-loop diagrams needed for the processes considered by the Dubna group in the past [3]–[6] in connection with theoretical support of experiments at CERN and DESY. The **FORM** codes (at present **FORM3** [7] is being used) computing the one-loop ultraviolet finite scalar form factors of the amplitudes of the decays $Z(H, W) \rightarrow f\bar{f}$ were unified and put into a special program environment, written in **JAVA**. This version was used for a revision of Atomic Parity Violation [8], and for a calculation of the one-loop electroweak radiative corrections for the process $e^+e^- \rightarrow f\bar{f}$ [9] and neutrino DIS [10].

In the second phase of the project (2004–2006), we extend automatic calculations of such a kind to a large number of HEP processes, with emphasis on LHC physics.

Present status

The present level of the system is realized in the version **v1.00**. This version has a fresh new layout and is more user friendly than earlier versions.

New in version **1.00** are Compton scattering and several other $f\bar{f}bb$ processes. By our philosophy we treat them as building blocks for future calculations of $5 \rightarrow 0$ processes (fully massive case).

For the last year we substantially enhanced our computer system compared to the status presented in the years 2002–2003 at large-scale international conferences, such as ACAT2002 [11]–[14], ICHEP2002 [15], RADCOR2002 [16] and Workshops at Saint-Malo [17], CERN [18], Montpellier [19] and Paris [20].

How to get started and use SANC

To learn more about available **SANC** servers look at our home pages at Dubna <http://sanc.jinr.ru> or CERN <http://pcphysanc.cern.ch>.

SANC may be accessed via the so called **SANC** client — a software free to download. The user will always get the latest (updates) versions from either of the two above addresses.

Levels of the calculations

SANC is subdivided into three logical levels, each with a specific purpose.

- Level 1, Analytic

The analytical application includes enhanced tools of **FORM** procedures. **SANC** has three types of procedures: *specific*, *intrinsic* and *special*. The specific procedures are used by **FORM** source codes, typically only once; they are always visible (see Section 3) and can be modified by the user. The action of intrinsic procedures is uniquely specified by their arguments, therefore they may be used by many **FORM** codes. Their bodies are not accessible to the users. Finally, special procedures are used only a few number of

times to perform some special action in a given **FORM** code. Normally, they have very simple arguments like field indices.

The Figures 2–3 show fully open menus for “Precomputation” and for available “Processes” in the QED part, Fig 18, and “Processes” in the EW part, Fig. 19. In this article we explain in detail the process of “Precomputation” .

Entering your chosen process, you are in an active session and receive the analytical result for scalar Form Factors (FF), Helicity Amplitudes (HA) and the accompanying Bremsstrahlung contributions (BR).

For the calculation of the HAs we use techniques of Vega–Wudka [21] and Kleiss–Stirling [22].

As a main example of the description of the calculation of FF and HA for processes $f_1 \bar{f}_1 \rightarrow f \bar{f}$ we mention Ref. [9]. All calculations of FF→HA→BR on the **SANC** tree are realized in the same job stream.

- Level 2, Numerical

The analytic results are transferred to the second level where they are analyzed by a software package **s2n.f** (*symbols-to-numbers*), written in PERL. The **s2n.f** package automatically generates **FORTRAN** codes for subsequent numerical computations of decay rates and process cross sections. The calculational flow inside levels 1 and 2 and the exchange of data between them is fully automatized and is governed by selecting corresponding items in menus.

The **s2n** part of the **SANC** system is completely fixed for all available decays (besides $(Z \rightarrow W^+ W^-)$; for NC $4f \rightarrow 0$ processes we have **s2n** for FF→HA→SoftBR parts, and for CC processes $f_1 \bar{f}_1' \rightarrow f_1' \bar{f}_1''$ we have **s2n** for FF→HA→ SoftBR+HardBR parts (here f_1 with or without primes denotes massless fermions, *e.g.* of the 1st generation). We have performed many high-precision comparisons of the numerical results derived with the aid of **s2n.f** with the results of the alternative systems **FeynArts** [23] and **GRACE** [24] and the code **topfit** [25].

- Level 3, MC generators

In **version 1.00**, MC generators are available only for $B \rightarrow f \bar{f}$ decays together with relevant graphic interface. The results can be presented in a variety of histograms. The user may “play with the parameters” of histograms in the window.

A first Monte Carlo generator for decays $Z(H, W) \rightarrow f \bar{f} \gamma$ is created in close contact with members of the KK collaboration, see papers [26, 27]. The MC generator is also accessible via menus, therefore, for the case of decays we are able to demonstrate how *the full chain of calculations* works out within our integrated system. The MC event generators are supposed to be usable also in a “stand alone” mode ready to be incorporated into the software of experiments.

This paper is organized as follows:

In Section 2 we describe amplitudes for all available in **version 1.00** 3- and 4-leg processes.

Section 3, the main section of this paper, is fully devoted to the concept of precomputation; a comprehensive description of the **SANC** precomputation tree and its modules is given. We assume that while reading this part the reader will be looking inside the corresponding modules. For one example, namely precomputation of photonic vacuum polarization, we demonstrate the whole process of calculations by presenting intermediate results after each procedure is called.

In Section 4 we describe a part of **SANC** procedures, mostly those which are used by precomputation modules.

In Section 5 we briefly describe the **SANC** trees of processes implemented for the time being.

Although this paper is mostly devoted to the **SANC** precomputation, in Section 6 we give a short **User Guide** for **version 1.00**. A more detailed description of the **SANC** processes trees and computer aspects of **SANC** system will be given elsewhere.

2 Amplitude Basis, Scalar Form Factors, Helicity Amplitudes

2.1 Introduction

In this section we present a collection of formulae for the amplitudes of basic SM $1 \rightarrow 2$ decays and $2 \rightarrow 2$ processes available in **SANC** v.1.00. The *covariant one-loop amplitude* (CA) corresponds to a result of the straightforward standard calculation by means of **SANC** programs and procedures of *all* diagrams contributing to a given process at the tree (Born) and one-loop levels. It is represented in a certain *basis*, made of strings of Dirac matrices and/or external momenta (*structures*), contracted with polarization vectors of vector bosons, if any. We usually omit Dirac spinors. The amplitude also contains kinematical factors and coupling constants and is parameterized by a certain number of form factors, which we denote by \mathcal{F} , in general with an index labeling the corresponding structure. The number of FFs is equal to the number of structures. If there is only one FF, we normally do not label it. For the processes with non zero tree-level amplitudes the FFs have the form

$$\mathcal{F} = 1 + k\tilde{\mathcal{F}}, \quad (1)$$

where “1” is due to the Born level and the term $\tilde{\mathcal{F}}$ with the factor

$$k = \frac{g^2}{16\pi^2}, \quad (2)$$

is due to the one-loop level. We also use various coupling constants

$$Q_f, \quad I_f^{(3)}, \quad \sigma_f = v_f + a_f, \quad \delta_f = v_f - a_f, \quad s_w = \frac{e}{g}, \quad c_w = \frac{M_w}{M_z}, \quad etc. \quad (3)$$

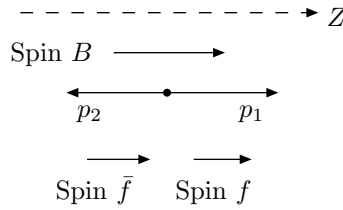
Given a CA parameterized by a certain number of FFs, **SANC** computes a set of HAs, denoted by $\mathcal{H}_{\lambda_1\lambda_2\lambda_3\dots}$, where $\lambda_1\lambda_2\lambda_3\dots$ denote the signs of particle spin projections onto a quantization axis as will be explained in the following sections.

In the representation of massive HAs, the following notation is very useful:

$$P^\pm(I, M_1, M_2) = \sqrt{|I - (M_1 \pm M_2)^2|}. \quad (4)$$

2.2 The 3-leg processes $B(Q) \rightarrow f(p_1) + \bar{f}(p_2)$

In this section we present amplitudes for $1 \rightarrow 2$ decays involving one vector boson and two fermions. For all $B \rightarrow f\bar{f}$ decays, except Higgs boson decay, the three λ_i in $\mathcal{H}_{\lambda_1\lambda_2\lambda_3}$ denote the signs of the boson, fermion and antifermion spin projections, respectively. Fermion spins are projected onto their momenta, the boson spin is projected onto the fermion momentum. For example, \mathcal{H}_{++-} corresponds to the following spin configuration:



- $H \rightarrow f + \bar{f}$

Its CA is described by one FF only:

$$\mathcal{A}_{Hff} = \left(-\frac{g}{2} \frac{m_f}{M_W} \right) \mathcal{F}_S. \quad (5)$$

Correspondingly, there is only one independent HA:

$$\begin{aligned} \mathcal{H}_{++} &= \mathcal{H}_{--} = \frac{g}{2} \frac{m_f}{M_W} P_{Hff}^+ \mathcal{F}_S, \\ \mathcal{H}_{+-} &= \mathcal{H}_{-+} = 0, \end{aligned} \quad (6)$$

here

$$P_{Hff}^+ = P^+ (M_H^2, m_f, m_f) = \sqrt{M_H^2 - 4m_f^2}. \quad (7)$$

- $V \rightarrow f + \bar{f}$

The CA of the decay of a heavy vector particle (V) contains two FFs:

$$\mathcal{A}_{Vff} = eQ_f [i\gamma_\mu \mathcal{F}_Q + m_f D_\mu \mathcal{F}_D] \epsilon_\mu(Q), \quad (8)$$

here and below in this section, until stated otherwise, $D_\mu = (p_2 - p_1)_\mu$.

The two independent HAs are:

$$\begin{aligned} \mathcal{H}_{++-} &= \mathcal{H}_{--+} = \sqrt{2} e Q_f M_V \mathcal{F}_Q, \\ \mathcal{H}_{0++} &= \mathcal{H}_{0--} = e m_f Q_f \left[(P_{Vff}^+)^2 \mathcal{F}_D + 2\mathcal{F}_Q \right], \\ \mathcal{H}_{+\pm+} &= \mathcal{H}_{\pm--} = \mathcal{H}_{0+-} = \mathcal{H}_{0-+} = \mathcal{H}_{-++} = \mathcal{H}_{-+-} = 0, \end{aligned} \quad (9)$$

$$P_{Vff}^+ = P^+ (M_V^2, m_f, m_f) = \sqrt{M_V^2 - 4m_f^2}. \quad (10)$$

- $Z \rightarrow f + \bar{f}$

In this case, the CA is described by three FFs:

$$\mathcal{A}_{Zff} = \frac{g}{2c_W} \left[i\gamma_\mu \gamma_6 I_f^{(3)} \mathcal{F}_L + i\gamma_\mu \delta_f \mathcal{F}_Q + m_f D_\mu I_f^{(3)} \mathcal{F}_D \right] \epsilon_\mu(Q), \quad (11)$$

where $\gamma_6, \gamma_7 = 1 \pm \gamma_5$. The three independent HAs look as follows:

$$\begin{aligned} \mathcal{H}_{++-} &= \frac{g}{\sqrt{2}c_W} \left[I_f^{(3)} (M_Z - P_{Zff}^+) \mathcal{F}_L + \delta_f M_Z \mathcal{F}_Q \right], \\ \mathcal{H}_{--+} &= \frac{g}{\sqrt{2}c_W} \left[I_f^{(3)} (M_Z + P_{Zff}^+) \mathcal{F}_L + \delta_f M_Z \mathcal{F}_Q \right], \\ \mathcal{H}_{0--} &= \mathcal{H}_{0++} = \frac{gm_f}{c_W} \left[I_f^{(3)} \mathcal{F}_L + \delta_f \mathcal{F}_Q + \frac{1}{2} I_f^{(3)} (P_{Zff}^+)^2 \mathcal{F}_D \right], \\ \mathcal{H}_{+\pm+} &= \mathcal{H}_{\pm--} = \mathcal{H}_{0+-} = \mathcal{H}_{0-+} = \mathcal{H}_{-++} = \mathcal{H}_{-+-} = 0, \end{aligned} \quad (12)$$

$$P_{Zff}^+ = P^+ (M_Z^2, m_f, m_f) = \sqrt{M_Z^2 - 4m_f^2}. \quad (13)$$

- $W^+ \rightarrow u + \bar{d}$ ($W^- \rightarrow \bar{u} + d$)

The CA of this decay is described by four FFs:

$$\mathcal{A}_{Wu\bar{d}} = \frac{g}{2\sqrt{2}} \left[i\gamma_\mu \gamma_6 \mathcal{F}_L + i\gamma_\mu \gamma_7 \mathcal{F}_R + D_\mu \gamma_6 \mathcal{F}_{LD} + D_\mu \gamma_7 \mathcal{F}_{RD} \right] \epsilon_\mu(Q). \quad (14)$$

The corresponding HAs read:

$$\begin{aligned} \mathcal{H}_{--+} &= \frac{g}{2} \left[(P_{Wud}^- + P_{Wud}^+) \mathcal{F}_L + (P_{Wud}^- - P_{Wud}^+) \mathcal{F}_R \right], \\ \mathcal{H}_{++-} &= \frac{g}{2} \left[(P_{Wud}^- - P_{Wud}^+) \mathcal{F}_L + (P_{Wud}^- + P_{Wud}^+) \mathcal{F}_R \right], \\ \mathcal{H}_{0++} &= \frac{g}{2\sqrt{2}} \frac{1}{M_W} \left[(P_{Wud}^- m_{u+d} + P_{Wud}^+ m_{u-d}) \mathcal{F}_L + (P_{Wud}^- m_{u+d} - P_{Wud}^+ m_{u-d}) \mathcal{F}_R \right. \\ &\quad \left. + P_{Wud}^+ P_{Wud}^- [P_{Wud}^+ + P_{Wud}^-] \mathcal{F}_{LD} + P_{Wud}^+ P_{Wud}^- [P_{Wud}^+ - P_{Wud}^-] \mathcal{F}_{RD} \right], \\ \mathcal{H}_{0--} &= \frac{g}{2\sqrt{2}} \frac{1}{M_W} \left[(P_{Wud}^- m_{u+d} - P_{Wud}^+ m_{u-d}) \mathcal{F}_L + (P_{Wud}^- m_{u+d} + P_{Wud}^+ m_{u-d}) \mathcal{F}_R \right. \\ &\quad \left. + P_{Wud}^+ P_{Wud}^- (P_{Wud}^+ - P_{Wud}^-) \mathcal{F}_{LD} + P_{Wud}^+ P_{Wud}^- (P_{Wud}^+ + P_{Wud}^-) \mathcal{F}_{RD} \right], \\ \mathcal{H}_{+\pm+} &= \mathcal{H}_{\pm--} = \mathcal{H}_{0+-} = \mathcal{H}_{0-+} = \mathcal{H}_{-+\pm} = 0, \end{aligned} \quad (15)$$

where

$$P_{Wud}^\pm = P(M_W^2, m_u, \pm m_d) = \sqrt{M_W^2 - m_{u\pm d}^2}, \quad m_{u\pm d} = m_u \pm m_d. \quad (16)$$

- $t \rightarrow b + W^+$

The CA has the same structure as in Eq. (14), but here with $D_\mu = (p_1 + p_2)_\mu$.

The four HAs are:

$$\begin{aligned} \mathcal{H}_{+-+} &= \frac{g}{2} \left[(P_{twb}^+ + P_{twb}^-) \mathcal{F}_L - (P_{twb}^+ - P_{twb}^-) \mathcal{F}_R \right], \\ \mathcal{H}_{-+-} &= -\frac{g}{2} \left[(P_{twb}^+ - P_{twb}^-) \mathcal{F}_L - (P_{twb}^+ + P_{twb}^-) \mathcal{F}_R \right], \\ \mathcal{H}_{++0} &= \frac{g}{2\sqrt{2}M_W} \left[(P_{twb}^+ m_{t-b} - P_{twb}^- m_{t+b}) \mathcal{F}_L - (P_{twb}^+ m_{t-b} + P_{twb}^- m_{t+b}) \mathcal{F}_R \right. \\ &\quad \left. + P_{twb}^+ P_{twb}^- (P_{twb}^- + P_{twb}^+) \mathcal{F}_{LD} - P_{twb}^+ P_{twb}^- (P_{twb}^- - P_{twb}^+) \mathcal{F}_{RD} \right], \\ \mathcal{H}_{--0} &= -\frac{g}{2\sqrt{2}M_W} \left[(P_{twb}^+ m_{t-b} + P_{twb}^- m_{t+b}) \mathcal{F}_L - (P_{twb}^+ m_{t-b} - P_{twb}^- m_{t+b}) \mathcal{F}_R \right. \\ &\quad \left. + P_{twb}^+ P_{twb}^- (P_{twb}^- - P_{twb}^+) \mathcal{F}_{LD} - P_{twb}^+ P_{twb}^- (P_{twb}^- + P_{twb}^+) \mathcal{F}_{RD} \right], \\ \mathcal{H}_{++\pm} &= \mathcal{H}_{+-0} = \mathcal{H}_{+--} = \mathcal{H}_{-++} = \mathcal{H}_{-+0} = \mathcal{H}_{--\pm} = 0, \end{aligned} \quad (17)$$

where

$$P_{twb}^\pm = P(M_W^2, m_t \pm m_b) = \sqrt{m_{t\pm b}^2 - M_W^2}, \quad m_{t\pm b} = m_t \pm m_b. \quad (18)$$

- $\bar{t} \rightarrow \bar{b} + W^-$

The amplitudes of this process are similar to the previous one (though not identical). Their explicit expressions can be found in the relevant module of the **SANC** tree.

2.3 The 3-leg processes $B(Q) \rightarrow V(p_1) + V(p_2)$, $V = \gamma, Z, W$

In this section we just list CAs and HAs for basic three-boson decays in the SM. Note, the first two decays do not proceed at the tree level, this is why their FFs do not start with “1”.

- $H \rightarrow \gamma(p_1) + \gamma(p_2)$

$$\mathcal{A}_{H\gamma\gamma} = i k g s_W^2 \left(\delta_{\mu\nu} + 2 \frac{p_{1\mu} p_{2\nu}}{M_H^2} \right) \epsilon_\nu(p_1) \epsilon_\mu(p_2) \tilde{\mathcal{F}}, \quad (19)$$

$$\begin{aligned} \mathcal{H}_{++} &= \mathcal{H}_{--} = k g s_W^2 \tilde{\mathcal{F}}, \\ \mathcal{H}_{+-} &= \mathcal{H}_{-+} = 0. \end{aligned} \quad (20)$$

- $H \rightarrow Z(p_1) + \gamma(p_2)$

$$\mathcal{A}_{H\gamma Z} = i k g s_W \left[\left(1 - \frac{M_Z^2}{M_H^2} \right) \delta_{\mu\nu} + 2 \frac{p_{1\mu} p_{2\nu}}{M_H^2} \right] \epsilon_\nu(p_1) \epsilon_\mu(p_2) \tilde{\mathcal{F}}, \quad (21)$$

$$\begin{aligned} \mathcal{H}_{++} &= \mathcal{H}_{--} = k g s_W \left(1 - \frac{M_Z^2}{M_H^2} \right) \tilde{\mathcal{F}}, \\ \mathcal{H}_{+-} &= \mathcal{H}_{0\pm} = \mathcal{H}_{-+} = 0. \end{aligned} \quad (22)$$

- $H \rightarrow Z(p_1) + Z(p_2)$

$$\mathcal{A}_{HZZ} = \left(-\frac{g M_Z}{c_W} \right) \left(\delta_{\mu\nu} \mathcal{F}_D + \frac{p_{1\mu} p_{2\nu}}{M_H^2} \mathcal{F}_P \right) \epsilon_\nu(p_1) \epsilon_\mu(p_2), \quad (23)$$

$$\begin{aligned} \mathcal{H}_{++} &= \mathcal{H}_{--} = \left(-\frac{g M_Z}{c_W} \right) \mathcal{F}_D, \\ \mathcal{H}_{00} &= \left(-\frac{g M_Z}{c_W} \right) \left[\left(1 - \frac{1}{2} \frac{M_H^2}{M_Z^2} \right) \mathcal{F}_D - \left(1 - \frac{1}{4} \frac{M_H^2}{M_Z^2} \right) \mathcal{F}_P \right], \\ \mathcal{H}_{\pm 0} &= \mathcal{H}_{+-} = \mathcal{H}_{0\pm} = \mathcal{H}_{-+} = 0. \end{aligned} \quad (24)$$

- $H \rightarrow W(p_1) + W(p_2)$

$$\mathcal{A}_{HWW} = (-g M_W) \left(\delta_{\mu\nu} \mathcal{F}_D + \frac{p_{1\mu} p_{2\nu}}{M_H^2} \mathcal{F}_P \right) \epsilon_\nu(p_1) \epsilon_\mu(p_2), \quad (25)$$

$$\begin{aligned} \mathcal{H}_{++} &= \mathcal{H}_{--} = (-g M_W) \mathcal{F}_D, \\ \mathcal{H}_{00} &= (-g M_W) \left[\left(1 - \frac{1}{2} \frac{M_H^2}{M_W^2} \right) \mathcal{F}_D - \left(1 - \frac{1}{4} \frac{M_H^2}{M_W^2} \right) \mathcal{F}_P \right], \\ \mathcal{H}_{+0} &= \mathcal{H}_{+-} = \mathcal{H}_{0+} = \mathcal{H}_{0-} = \mathcal{H}_{-+} = \mathcal{H}_{-0} = 0. \end{aligned} \quad (26)$$

- $Z(Q) \rightarrow W(p_1) + W(p_2)$

$$\begin{aligned} \mathcal{A}_{ZWW} &= i g c_W \left(p_{1\mu} p_{2\nu} D_\alpha \mathcal{F}_{D12} + \delta_{\alpha\nu} p_{1\mu} \mathcal{F}_{D1} + \delta_{\alpha\mu} p_{2\nu} \mathcal{F}_{D2} \right. \\ &\quad \left. + \delta_{\mu\nu} D_\alpha \mathcal{F}_{Dd} + \epsilon_{\beta\alpha\mu\nu} D_\beta \mathcal{F}_{D\epsilon}^{\text{fer}} \right) \epsilon_\alpha(Q) \epsilon_\nu(p_1) \epsilon_\mu(p_2). \end{aligned} \quad (27)$$

The HAs for this decay are not implemented in **SANC v.1.00**.

2.4 The 4-leg NC processes $f_1 \bar{f}_1 \rightarrow (\gamma Z) \rightarrow f \bar{f}$

Here we present the CAs and HAs for any $f_1 \bar{f}_1 f \bar{f} \rightarrow 0$ NC process at any channel s , t or u . Here 0 stands for *vacuum*, and by f_1 we mean a first generation fermion with field index 11,12,13,14, whose mass is neglected everywhere except in arguments of logs (mass singularities) and by f we mean any fermion with field indices from 11 to 22 (see Section 6 for definition of field indices). For such a case, the Higgs and ϕ^0 boson interactions with the f_1 current are also neglected.

The covariant one-loop amplitude of the $2f \rightarrow 2f$ process

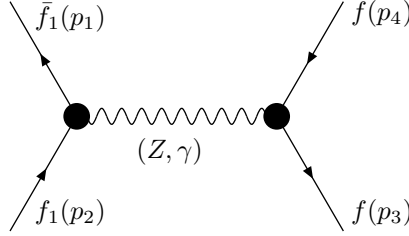


Figure 1: $f_1 \bar{f}_1 \rightarrow f \bar{f}$ process.

is described in terms of six form factors: LL, QL, LQ, QQ, LD and QD , corresponding to six Dirac structures (\mathcal{A}_γ is also described by a QQ structure, it is separated out for convenience; $\alpha(s) = \alpha(0)\mathcal{F}_\gamma(s)$). Note that all 4-momenta are incoming and the usual Mandelstam invariants in our metric (i.e. $p^2 = -m^2$) are:

$$(p_1 + p_2)^2 = -s, \quad (p_2 + p_3)^2 = -t, \quad (p_2 + p_4)^2 = -u. \quad (28)$$

The γ and Z exchange amplitudes are:

$$\mathcal{A}_\gamma(s) = i e^2 \frac{Q_{f_1} Q_f}{s} \mathcal{F}_\gamma(s) \gamma_\mu \otimes \gamma_\mu, \quad (29)$$

$$\begin{aligned} \mathcal{A}_Z(s) = & i e^2 \frac{\chi_Z(s)}{s} \\ & \times \left\{ I_{f_1}^{(3)} I_f^{(3)} \gamma_\mu (1 + \gamma_5) \otimes \gamma_\mu (1 + \gamma_5) \mathcal{F}_{LL}(s, t, u) + \delta_{f_1} I_f^{(3)} \gamma_\mu \otimes \gamma_\mu (1 + \gamma_5) \mathcal{F}_{QL}(s, t, u) \right. \\ & + I_{f_1}^{(3)} \delta_f \gamma_\mu (1 + \gamma_5) \otimes \gamma_\mu \mathcal{F}_{LQ}(s, t, u) + \delta_{f_1} \delta_f \gamma_\mu \otimes \gamma_\mu \mathcal{F}_{QQ}(s, t, u) \\ & \left. + I_{f_1}^{(3)} I_f^{(3)} \gamma_\mu (1 + \gamma_5) \otimes (-im_f D_\mu) \mathcal{F}_{LD}(s, t, u) + \delta_{f_1} I_f^{(3)} \gamma_\mu \otimes (-im_f D_\mu) \mathcal{F}_{QD}(s, t, u) \right\}. \end{aligned} \quad (30)$$

Here and below in this and in the next sections, $D_\mu = (p_4 - p_3)_\mu$ and $\chi_Z(s)$ is the Z/γ propagator ratio

$$\chi_Z(s) = \frac{1}{4s_W^2 c_W^2} \frac{s}{s - M_Z^2 + iM_Z \Gamma_Z}. \quad (31)$$

Symbol $\gamma_\mu \otimes \gamma_\mu$ is used in the following short-hand notation:

$$\gamma_\mu \otimes \gamma_\nu = \bar{v}(p_1) \gamma_\mu u(p_2) \bar{u}(p_3) \gamma_\nu v(p_4). \quad (32)$$

For more details see Ref. [9].

If the f_1 mass is neglected, we have six corresponding HAs. They depend on kinematical variables, coupling constants and our six scalar form factors:

$$\begin{aligned}
\mathcal{H}_{-++-} &= -e^2 (1 + \cos \vartheta) \left(Q_{f_1} Q_f \mathcal{F}_\gamma(s) + \chi_Z(s) \delta_{f_1} \left[\left(1 - \frac{P^+}{\sqrt{s}} \right) I_f^{(3)} \mathcal{F}_{QL} + \delta_f \mathcal{F}_{QQ} \right] \right), \\
\mathcal{H}_{-+-+} &= -e^2 (1 - \cos \vartheta) \left(Q_{f_1} Q_f \mathcal{F}_\gamma(s) + \chi_Z(s) \delta_{f_1} \left[\left(1 + \frac{P^+}{\sqrt{s}} \right) I_f^{(3)} \mathcal{F}_{QL} + \delta_f \mathcal{F}_{QQ} \right] \right), \\
\mathcal{H}_{-+--} &= \mathcal{H}_{-+++} = e^2 \frac{2m_f}{\sqrt{s}} \sin \vartheta \left(Q_{f_1} Q_f \mathcal{F}_\gamma(s) \right. \\
&\quad \left. + \chi_Z(s) \delta_{f_1} \left[I_f^{(3)} \mathcal{F}_{QL} + \delta_f \mathcal{F}_{QQ} + \frac{1}{2} (P^+)^2 I_f^{(3)} \mathcal{F}_{QD} \right] \right), \\
\mathcal{H}_{+--+} &= \mathcal{H}_{+---} = -e^2 \frac{2m_f}{\sqrt{s}} \sin \vartheta \left(Q_{f_1} Q_f \mathcal{F}_\gamma(s) + \chi_Z(s) \left[2I_{f_1}^{(3)} I_f^{(3)} \mathcal{F}_{LL} + 2I_{f_1}^{(3)} \delta_f \mathcal{F}_{LQ} \right. \right. \\
&\quad \left. \left. + \delta_{f_1} I_f^{(3)} \mathcal{F}_{QL} + \delta_{f_1} \delta_f \mathcal{F}_{QQ} + \frac{1}{2} (P^+)^2 I_f^{(3)} \left(2I_{f_1}^{(3)} \mathcal{F}_{LD} + \delta_{f_1} \mathcal{F}_{QD} \right) \right] \right), \\
\mathcal{H}_{+-+-} &= -e^2 (1 - \cos \vartheta) \left(Q_{f_1} Q_f \mathcal{F}_\gamma(s) + \chi_Z(s) \left[\left(1 - \frac{P^+}{\sqrt{s}} \right) I_f^{(3)} \left(2I_{f_1}^{(3)} \mathcal{F}_{LL} + \delta_{f_1} \mathcal{F}_{QL} \right) \right. \right. \\
&\quad \left. \left. + \delta_f \left(2I_{f_1}^{(3)} \mathcal{F}_{LQ} + \delta_{f_1} \mathcal{F}_{QQ} \right) \right] \right), \\
\mathcal{H}_{+---} &= -e^2 (1 + \cos \vartheta) \left(Q_{f_1} Q_f \mathcal{F}_\gamma(s) + \chi_Z(s) \left[\left(1 + \frac{P^+}{\sqrt{s}} \right) I_f^{(3)} \left(2I_{f_1}^{(3)} \mathcal{F}_{LL} + \delta_{f_1} \mathcal{F}_{QL} \right) \right. \right. \\
&\quad \left. \left. + \delta_f \left(2I_{f_1}^{(3)} \mathcal{F}_{LQ} + \delta_{f_1} \mathcal{F}_{QQ} \right) \right] \right), \\
\mathcal{H}_{++++} &= \mathcal{H}_{++-+} = \mathcal{H}_{--++} = \mathcal{H}_{----} = 0;
\end{aligned} \tag{33}$$

helicity indices, for example, $+-+ -$ denote the signs of the fermion spin projections onto their momenta p_1, p_2, p_3, p_4 , respectively.

Moreover,

$$P^+ = P^+(s, m_f, m_f) = \sqrt{s - 4m_f^2}, \tag{34}$$

and the scattering angle $\cos \vartheta$ is connected to the invariant t :

$$\cos \vartheta = \left(t - m_f^2 + \frac{s}{2} \right) \frac{2}{s\beta_f}, \tag{35}$$

where

$$\beta_f = \sqrt{1 - \frac{4m_f^2}{s}}. \tag{36}$$

2.5 The 4-leg CC processes $f_1 \bar{f}'_1 \rightarrow (W) \rightarrow f \bar{f}'$

In version 1.00 we have implemented particular $2f \rightarrow 2f$ CC processes, having in mind their application to Drell–Yan type CC processes at hadron colliders as well as for 3-particle top decays.

- $\bar{u} + d \rightarrow l^- + \bar{\nu}_l$

$$\begin{aligned} \mathcal{A}_{W-} &= i e^2 \frac{\chi_W(s)}{4s} \left[\gamma_\mu (1 + \gamma_5) \otimes \gamma_\mu (1 + \gamma_5) \mathcal{F}_{LL}(s, t, u) \right. \\ &\quad \left. + \gamma_\mu (1 + \gamma_5) \otimes (1 + \gamma_5) (-iD_\mu) \mathcal{F}_{LD}(s, t, u) \right]. \end{aligned} \quad (37)$$

There are only two non-zero HAs for the case when only one mass (lepton) is not neglected:

$$\begin{aligned} \mathcal{H}_{+---} &= -e^2 (1 + \cos \vartheta_{dl}) \frac{P^+}{\sqrt{s}} \chi_W(s) \mathcal{F}_{LL}(s, t, u), \\ \mathcal{H}_{+-++} &= -e^2 \sin \vartheta_{dl} P^+ \chi_W(s) \left[\frac{m_l}{s} \mathcal{F}_{LL}(s, t, u) + \left(1 - \frac{m_l^2}{s} \right) \mathcal{F}_{LD}(s, t, u) \right], \\ \mathcal{H}_{++++} &= \mathcal{H}_{++-+} = \mathcal{H}_{+-+-} = \mathcal{H}_{-+++} = \mathcal{H}_{-+-+} = \mathcal{H}_{--++} = \mathcal{H}_{----} = 0, \end{aligned} \quad (38)$$

here and below

$$P^+ = P^+(s, m_l, 0) = \sqrt{s - m_l^2}. \quad (39)$$

- $\bar{d} + u \rightarrow l^+ + \nu_l$

$$\begin{aligned} \mathcal{A}_{W+} &= i e^2 \frac{\chi_W(s)}{4s} \left[\gamma_\mu (1 + \gamma_5) \otimes \gamma_\mu (1 + \gamma_5) \mathcal{F}_{LL}(s, t, u) \right. \\ &\quad \left. + \gamma_\mu (1 + \gamma_5) \otimes (1 - \gamma_5) (-iD_\mu) \mathcal{F}_{RD}(s, t, u) \right], \end{aligned} \quad (40)$$

$$\begin{aligned} \mathcal{H}_{+---} &= -e^2 (1 + \cos \vartheta_{uv}) \frac{P^+}{\sqrt{s}} \chi_W(s) \mathcal{F}_{LL}(s, t, u), \\ \mathcal{H}_{+----} &= -e^2 \sin \vartheta_{uv} P^+ \chi_W(s) \left[\frac{m_l}{s} \mathcal{F}_{LL}(s, t, u) + \left(1 - \frac{m_l^2}{s} \right) \mathcal{F}_{RD}(s, t, u) \right], \\ \mathcal{H}_{++++} &= \mathcal{H}_{++-+} = \mathcal{H}_{+-++} = \mathcal{H}_{-+++} = \mathcal{H}_{-+-+} = \mathcal{H}_{--++} = \mathcal{H}_{----} = 0. \end{aligned} \quad (41)$$

Note our angle convention: ϑ_{dl} and ϑ_{uv} are chosen to be the angles between *particle momenta* in the initial and final states in the cms reference frame, and here

$$\chi_W(s) = \frac{s}{2s_W^2} \frac{1}{s - M_W^2 + iM_W \Gamma_W}. \quad (42)$$

- $t(p_2) \rightarrow b(p_1) + l^+(p_4) + \nu_l(p_3)$

For this case there are four different structures and scalar form factors if the mass of the b quark is not neglected. The CA reads:

$$\begin{aligned} \mathcal{A}_t &= i e^2 \frac{d_W(s)}{4} \left[\gamma_\mu (1 + \gamma_5) \otimes \gamma_\mu (1 + \gamma_5) \mathcal{F}_{LL}(s, t) \right. \\ &\quad + \gamma_\mu (1 - \gamma_5) \otimes \gamma_\mu (1 + \gamma_5) \mathcal{F}_{RL}(s, t) \\ &\quad + (1 + \gamma_5) \otimes \gamma_\mu (1 + \gamma_5) (-iD_\mu) \mathcal{F}_{LD}(s, t) \\ &\quad \left. + (1 - \gamma_5) \otimes \gamma_\mu (1 + \gamma_5) (-iD_\mu) \mathcal{F}_{RD}(s, t) \right]. \end{aligned} \quad (43)$$

Here D_μ and 4-momentum conservation read:

$$D_\mu = (p_1 + p_2)_\mu, \quad p_2 = p_1 + p_3 + p_4, \quad (44)$$

while the invariants are

$$s = -(p_3 + p_4)^2, \quad t = -(p_1 + p_4)^2, \quad (45)$$

and

$$d_W(s) = \frac{1}{2s_W^2} \frac{1}{s - M_W^2 + iM_W\Gamma_W}. \quad (46)$$

The four non-zero HAs are:

$$\begin{aligned} \mathcal{H}_{++++} &= +\frac{1}{2} e^2 d_W(s) \sin \vartheta_l \left\{ (P^+ m_{t-b} - P^- m_{t+b}) \mathcal{F}_{LL} - (P^+ m_{t-b} + P^- m_{t+b}) \mathcal{F}_{RL} \right. \\ &\quad \left. - P^+ P^- \left[(P^+ + P^-) \mathcal{F}_{LD} + (P^+ - P^-) \mathcal{F}_{RD} \right] \right\}, \\ \mathcal{H}_{----+} &= -\frac{1}{2} e^2 d_W(s) \sin \vartheta_l \left\{ (P^+ m_{t-b} + P^- m_{t+b}) \mathcal{F}_{LL} - (P^+ m_{t-b} - P^- m_{t+b}) \mathcal{F}_{RL} \right. \\ &\quad \left. + P^+ P^- \left[(P^+ - P^-) \mathcal{F}_{LD} + (P^+ + P^-) \mathcal{F}_{RD} \right] \right\}, \\ \mathcal{H}_{+---+} &= +\frac{1}{2} e^2 d_W(s) (1 - \cos \vartheta_l) \sqrt{s} \left\{ (P^+ - P^-) \mathcal{F}_{LL} - (P^+ + P^-) \mathcal{F}_{RL} \right\}, \\ \mathcal{H}_{-++-+} &= -\frac{1}{2} e^2 d_W(s) (1 + \cos \vartheta_l) \sqrt{s} \left\{ (P^+ + P^-) \mathcal{F}_{LL} - (P^+ - P^-) \mathcal{F}_{RL} \right\}. \end{aligned} \quad (47)$$

Here

$$P^\pm = \sqrt{(m_t \pm m_b)^2 - s}. \quad (48)$$

Finally, ϑ_l is the angle between leptonic 4-momentum in R-frame ($\vec{p}_3 + \vec{p}_4 = 0$) and the z-axis is chosen along p_1 momentum in the rest frame of decaying top. It is related to t invariant by

$$t = m_b^2 + \frac{1}{2} \left[m_t^2 - m_b^2 - s - \sqrt{\lambda(s, m_t^2, m_b^2)} \cos \vartheta_l \right], \quad (49)$$

where $\lambda(x, y, z)$ is the ordinary kinematical function

$$\lambda(x, y, z) = x^2 + y^2 + z^2 - 2xy - 2xz - 2yz. \quad (50)$$

- $\bar{t} \rightarrow \bar{b} + l^- + \bar{\nu}_l$

This case is similar, although not identical to the previous one. For exact expressions see relevant module in the SANC tree:

EW \rightarrow Processes \rightarrow 4 legs \rightarrow Charged Current \rightarrow $t \rightarrow b \, l \, \nu$ (HA).

2.6 Bhabha scattering

The CA for Bhabha scattering can be derived from Eqs.(29–30) as follows (if the electron mass is neglected):

$$\begin{aligned}
\mathcal{A}_{\text{Bhabha}} &= \mathcal{A}_\gamma(s) + \mathcal{A}_Z(s) - [\mathcal{A}_\gamma(t) + \mathcal{A}_Z(t)] \\
&= i e^2 \left[\gamma_\mu \otimes \gamma_\mu \frac{\mathcal{F}_\gamma(s)}{s} - \gamma_\mu \otimes \gamma_\mu \frac{\mathcal{F}_\gamma(t)}{t} \right] \\
&\quad + i e^2 \frac{\chi_Z(s)}{s} \\
&\quad \times \left\{ \left(I_e^{(3)} \right)^2 \gamma_\mu (1 + \gamma_5) \otimes \gamma_\mu (1 + \gamma_5) \mathcal{F}_{LL}(s, t, u) + \delta_e I_e^{(3)} \gamma_\mu \otimes \gamma_\mu (1 + \gamma_5) \mathcal{F}_{QL}(s, t, u) \right. \\
&\quad \left. + I_e^{(3)} \delta_e \gamma_\mu (1 + \gamma_5) \otimes \gamma_\mu \mathcal{F}_{LQ}(s, t, u) + \delta_e^2 \gamma_\mu \otimes \gamma_\mu \mathcal{F}_{QQ}(s, t, u) \right\} \\
&\quad - i e^2 \frac{\chi_Z(t)}{t} \\
&\quad \times \left\{ \left(I_e^{(3)} \right)^2 \gamma_\mu (1 + \gamma_5) \otimes \gamma_\mu (1 + \gamma_5) \mathcal{F}_{LL}(t, s, u) + \delta_e I_e^{(3)} \gamma_\mu \otimes \gamma_\mu (1 + \gamma_5) \mathcal{F}_{QL}(t, s, u) \right. \\
&\quad \left. + I_e^{(3)} \delta_e \gamma_\mu (1 + \gamma_5) \otimes \gamma_\mu \mathcal{F}_{LQ}(t, s, u) + \delta_e^2 \gamma_\mu \otimes \gamma_\mu \mathcal{F}_{QQ}(t, s, u) \right\}. \tag{51}
\end{aligned}$$

It is described by the electromagnetic running coupling constant and four FFs with exchanged arguments s and t .

There are six non-zero HAs:

$$\begin{aligned}
\mathcal{H}_{++++} &= -2e^2 \frac{s}{t} \left\{ \mathcal{F}_{QQ}^\gamma(t, s, u) - \chi_Z(t) \delta_e [\mathcal{F}_{QL}^Z(t, s, u) - \delta_e \mathcal{F}_{QQ}^Z(t, s, u)] \right\}, \\
\mathcal{H}_{----} &= -2e^2 \frac{s}{t} \left\{ \mathcal{F}_{QQ}^\gamma(t, s, u) - \chi_Z(t) \delta_e [\mathcal{F}_{LQ}^Z(t, s, u) - \delta_e \mathcal{F}_{QQ}^Z(t, s, u)] \right\}, \\
\mathcal{H}_{+-+-} &= -e^2 (1 - \cos \theta) \left\{ \mathcal{F}_{QQ}^\gamma(s, t, u) - \chi_Z(s) \delta_e [\mathcal{F}_{LQ}^Z(s, t, u) - \delta_e \mathcal{F}_{QQ}^Z(s, t, u)] \right\}, \\
\mathcal{H}_{-+-+} &= -e^2 (1 - \cos \theta) \left\{ \mathcal{F}_{QQ}^\gamma(s, t, u) - \chi_Z(s) \delta_e [\mathcal{F}_{QL}^Z(s, t, u) - \delta_e \mathcal{F}_{QQ}^Z(s, t, u)] \right\}, \\
\mathcal{H}_{+--+} &= -e^2 (1 + \cos \theta) \left\{ \mathcal{F}_{QQ}^\gamma(s, t, u) \right. \\
&\quad \left. + \chi_Z(s) (\mathcal{F}_{LL}^Z(s, t, u) - \delta_e [\mathcal{F}_{LQ}^Z(s, t, u) + \mathcal{F}_{QL}^Z(s, t, u) - \delta_e \mathcal{F}_{QQ}^Z(s, t, u)]) \right. \\
&\quad \left. + \frac{s}{t} [\mathcal{F}_{QQ}^\gamma(t, s, u) + \chi_Z(t) (\mathcal{F}_{LL}^Z(t, s, u) - \delta_e [\mathcal{F}_{LQ}^Z(t, s, u) + \mathcal{F}_{QL}^Z(t, s, u) - \delta_e \mathcal{F}_{QQ}^Z(t, s, u)])] \right\}, \\
\mathcal{H}_{-++-} &= -e^2 (1 + \cos \theta) \left\{ \mathcal{F}_{QQ}^\gamma(s, t, u) + \delta_e^2 \chi_Z(s) \mathcal{F}_{QQ}^Z(s, t, u) \right. \\
&\quad \left. + \frac{s}{t} [\mathcal{F}_{QQ}^\gamma(t, s, u) + \delta_e^2 \chi_Z(t) \mathcal{F}_{QQ}^Z(t, s, u)] \right\}, \\
\mathcal{H}_{++++} &= \mathcal{H}_{++-+} = \mathcal{H}_{+-++} = \mathcal{H}_{+---} = 0, \\
\mathcal{H}_{-+++} &= \mathcal{H}_{-+-+} = \mathcal{H}_{--++} = \mathcal{H}_{----+} = 0, \tag{52}
\end{aligned}$$

however, since for Bhabha scattering $\mathcal{F}_{LQ}^Z = \mathcal{F}_{QL}^Z$, the number of independent HAs is actually reduced to four as expected.

2.7 $f\bar{f}bb \rightarrow 0$ processes

In SANC v.1.00 we have implemented three classes of $f\bar{f}bb \rightarrow 0$ processes: $f\bar{f}\gamma\gamma \rightarrow 0$, $f\bar{f}Z\gamma \rightarrow 0$ and $f\bar{f}H\gamma \rightarrow 0$. Due to space shortage, we limit ourselves in this paper to the process $f\bar{f}H\gamma \rightarrow 0$. Moreover, for $f\bar{f}bb \rightarrow 0$ processes the variety of cross channels is more rich than for the case of $f\bar{f}ff \rightarrow 0$. For example, for process $f\bar{f}H\gamma \rightarrow 0$ it is worth considering at least three channels:

- annihilation, $f\bar{f} \rightarrow H\gamma$;
- decay, $H \rightarrow f\bar{f}\gamma$;
- and H production at γe colliders, $\gamma e \rightarrow He$.

For all the channels we still can write down almost unique CA. Below we give it exactly for the annihilation channel, $f(p_2)\bar{f}(p_1) \rightarrow H(p_4)\gamma(p_3)$, but it might be easily rewritten into any other channel. This is not the case, however, for the HAs. The latter must be recomputed for any given channel.

There are eight structures transverse in photonic 4-momentum, 4 vector and 4 axial ones

$$\begin{aligned}
\mathcal{A}_{f\bar{f}H\gamma} = & -e g \frac{Q_f m_f}{M_w} \left\{ \bar{v}(p_1) u(p_2) [(U^2 + m_f^2)(p_2)_\nu - (T^2 + m_f^2)(p_1)_\nu] \varepsilon_\nu^\gamma(p_3) F_{v1}(s, t) \right. \\
& - \bar{v}(p_1) \not{p}_3 \gamma_\nu u(p_2) \varepsilon_\nu^\gamma(p_3) F_{v2}(s, t) \\
& - \bar{v}(p_1) i \left[\not{p}_3(p_1)_\nu + \frac{1}{2}(U^2 + m_f^2)\gamma_\nu \right] u(p_2) \varepsilon_\nu^\gamma(p_3) F_{v3}(s, t) \\
& - \bar{v}(p_1) i \left[\not{p}_3(p_2)_\nu + \frac{1}{2}(T^2 + m_f^2)\gamma_\nu \right] u(p_2) \varepsilon_\nu^\gamma(p_3) F_{v4}(s, t) \\
& + \bar{v}(p_1) \gamma_5 u(p_2) [(U^2 + m_f^2)(p_2)_\nu - (T^2 + m_f^2)(p_1)_\nu] \varepsilon_\nu^\gamma(p_3) F_{a1}(s, t) \\
& - \bar{v}(p_1) \not{p}_3 \gamma_\nu \gamma_5 u(p_2) \varepsilon_\nu^\gamma(p_3) F_{a2}(s, t) \\
& - \bar{v}(p_1) i \left[\not{p}_3(p_1)_\nu + \frac{1}{2}(U^2 + m_f^2)\gamma_\nu \right] \gamma_5 u(p_2) \varepsilon_\nu^\gamma(p_3) F_{a3}(s, t) \\
& \left. - \bar{v}(p_1) i \left[\not{p}_3(p_2)_\nu + \frac{1}{2}(T^2 + m_f^2)\gamma_\nu \right] \gamma_5 u(p_2) \varepsilon_\nu^\gamma(p_3) F_{a4}(s, t) \right\}, \tag{53}
\end{aligned}$$

each multiplied by the corresponding FF: $F_{v1 \div v4}$ and $F_{a1 \div a4}$. In above expressions

$$T^2 = (p_2 + p_3)^2, \quad U^2 = (p_2 + p_4)^2. \tag{54}$$

The eight different HAs are

$$\begin{aligned}
\mathcal{H}_{+++} &= -k_0 \left[s\beta_f (\beta_f F_{v1}(s, t) - F_{a1}(s, t)) - \beta_+ (F_{v2}(s, t) - F_{a2}(s, t)) \right. \\
&\quad \left. + m_f (F_{v3}(s, t) - \beta_f F_{a3}(s, t)) + m_f (F_{v4}(s, t) + \beta_f F_{a4}(s, t)) \right], \\
\mathcal{H}_{---} &= k_0 \left[s\beta_f (\beta_f F_{v1}(s, t) + F_{a1}(s, t)) - \beta_+ (F_{v2}(s, t) + F_{a2}(s, t)) \right. \\
&\quad \left. + m_f (F_{v3}(s, t) + \beta_f F_{a3}(s, t)) + m_f (F_{v4}(s, t) - \beta_f F_{a4}(s, t)) \right], \\
\mathcal{H}_{++-} &= k_0 \left[s\beta_f (\beta_f F_{v1}(s, t) - F_{a1}(s, t)) - \beta_- (F_{v2}(s, t) + F_{a2}(s, t)) \right. \\
&\quad \left. + m_f (F_{v3}(s, t) - \beta_f F_{a3}(s, t)) + m_f (F_{v4}(s, t) - \beta_f F_{a4}(s, t)) \right],
\end{aligned}$$

$$\begin{aligned}
\mathcal{H}_{--+} &= -k_0 \left[s\beta_f (\beta_f F_{v1}(s, t) + F_{a1}(s, t)) - \beta_- (F_{v2}(s, t) - F_{a2}(s, t)) \right. \\
&\quad \left. + m_f (F_{v3}(s, t) + \beta_f F_{a3}(s, t)) + m_f (F_{v4}(s, t) - \beta_f F_{a4}(s, t)) \right], \\
\mathcal{H}_{++-} &= -k_+ \left[4\frac{m_f}{s} (F_{v2}(s, t) - F_{a2}(s, t)) \right. \\
&\quad \left. - \beta_+ (F_{v3}(s, t) + \beta_f F_{a3}(s, t)) - \beta_- (F_{v4}(s, t) + \beta_f F_{a4}(s, t)) \right], \\
\mathcal{H}_{+-+} &= -k_+ \left[4\frac{m_f}{s} (F_{v2}(s, t) + F_{a2}(s, t)) \right. \\
&\quad \left. - \beta_+ (F_{v3}(s, t) - \beta_f F_{a3}(s, t)) - \beta_- (F_{v4}(s, t) - \beta_f F_{a4}(s, t)) \right], \\
\mathcal{H}_{+--} &= -k_- \left[4\frac{m_f}{s} (F_{v2}(s, t) + F_{a2}(s, t)) \right. \\
&\quad \left. - \beta_- (F_{v3}(s, t) + \beta_f F_{a3}(s, t)) - \beta_+ (F_{v4}(s, t) + \beta_f F_{a4}(s, t)) \right], \\
\mathcal{H}_{-++} &= -k_- \left[4\frac{m_f}{s} (F_{v2}(s, t) - F_{a2}(s, t)) \right. \\
&\quad \left. - \beta_- (F_{v3}(s, t) - \beta_f F_{a3}(s, t)) - \beta_+ (F_{v4}(s, t) - \beta_f F_{a4}(s, t)) \right]
\end{aligned} \tag{55}$$

with the coefficients

$$\begin{aligned}
k_0 &= -e g \frac{Q_f m_f}{M_W} \frac{\sin \vartheta_\gamma}{2\sqrt{2}} (s - M_H^2), \\
k_\pm &= -e g \frac{Q_f m_f}{M_W} \frac{1 \pm \cos \vartheta_\gamma}{4\sqrt{2}} (s - M_H^2) \sqrt{s}.
\end{aligned} \tag{56}$$

Furthermore, β_f as in Eq. (36) and

$$\beta_\pm = 1 \pm \beta_f. \tag{57}$$

The angle ϑ_γ is the cms angle of the produced photon (angle between \vec{p}_2 and \vec{p}_3).

For the sake of completeness we also present the amplitude in the Born approximation. In terms of structures (53) it reads:

$$\begin{aligned}
\mathcal{A}_{ffH\gamma}^{Born} &= -e g \frac{Q_f m_f}{M_W} \frac{1}{(T^2 + m_f^2)(U^2 + m_f^2)} \\
&\quad \times \bar{v}(p_1) \left\{ [(U^2 + m_f^2)(p_2)_\nu - (T^2 + m_f^2)(p_1)_\nu] + \frac{1}{2}(Q^2 + M_H^2) \not{p}_3 \gamma_\nu \right\} u(p_2) \varepsilon_\nu^\gamma(p_3),
\end{aligned} \tag{58}$$

where

$$Q^2 = (p_1 + p_2)^2 = -s. \tag{59}$$

3 Precomputation

3.1 Introduction

This section is devoted to a rather detailed description of *precomputation* in **SANC**. The concept of precomputation is very important for the **SANC** project (see Ref. [2]). The basic idea here is to precompute as many one-loop diagrams and derived quantities (like renormalization constants, various building blocks *etc.*) as possible since the CPU time needed is in general quite large for the above quantities making it impractical to compute them in each **SANC** run.

Recall our particle notation conventions:

- f stands for any fermion (lepton or quark);
- b stands for neutral bosons A, Z, H ;
- when we need to be more concrete, we use l for leptons instead of f , and precisely A, Z, W, H for bosons.

It is worth emphasizing that at the precomputation phase it is not necessary to distinguish the process channel. While computing one-loop diagrams all 4-momenta are considered as incoming. In the derived expressions (say for the scalar form factors) any required channel is obtained by means of an appropriate permutation of arguments (say of Mandelstam variables s, t, u).

The Fig. 2 shows the fully open menu for “Precomputation” in the QED branch of **SANC**.

It consists of **Self** (Energies), **Vertex** and **Box** submenus. Self energies, in turn, are subdivided into **Photon** and **Lepton** submenus. They are further subdivided into calculation of diagrams themselves: **Photon Self** and **Lepton Self**. Precomputed and stored one-loop diagrams are used for calculation of corresponding renormalization constants: **CalcPhotRenConst** and **CalcLepRenConsts**, which are also stored. Altogether they are used for the calculation of renormalized propagators: **CalcPhotRenProp** and **CalcLepRenProp**. The latter is used to calculate the renormalized self energy 4-leg diagram for Compton scattering in QED **IIAA RenSelf**. The file **IIbb Bornlikeect** computes Born-like counterterms (see Section 3.2.3).

Vertex consists of 3-photon-leg **AAA**, photon-2 lepton **All** and 4-leg vertices for NC **IIAA** Compton-like QED processes (any channel, see Section 3.3.3).

Box is represented by the NC 2-photon exchange 4-lepton-leg box (direct and crossed) **IIII Box** (see Section 3.4.1) and by the two topologies (T2 and T4) of boxes appearing in Compton-like processes **IIAA Box** (see Section 3.4.2). Finally, the file **AA FF Box** transforms results obtained by **IIII Box** into the scalar form factors of a $4l$ process.

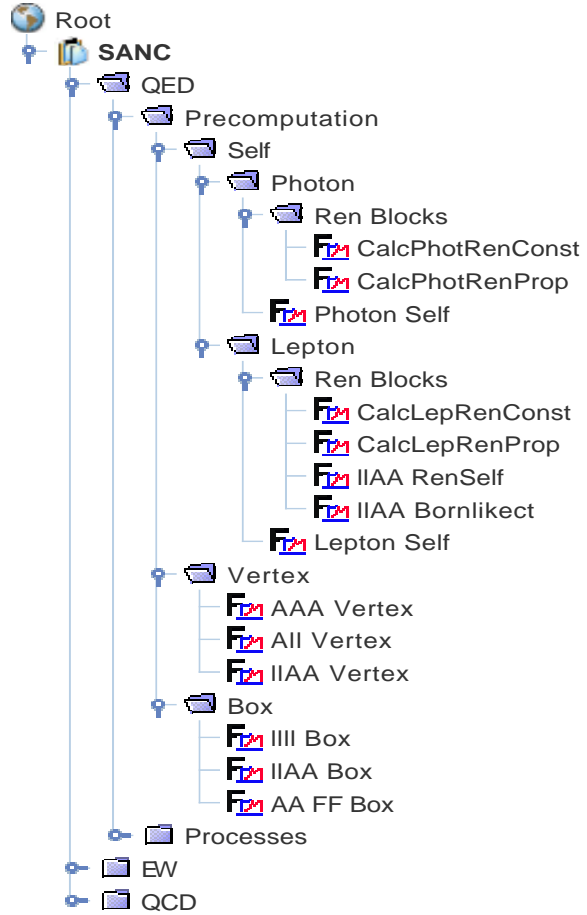


Figure 2: Precomputation in QED part.

The tree of “Precomputation” in the EW part, which is shown in Fig. 3, has many more branches.

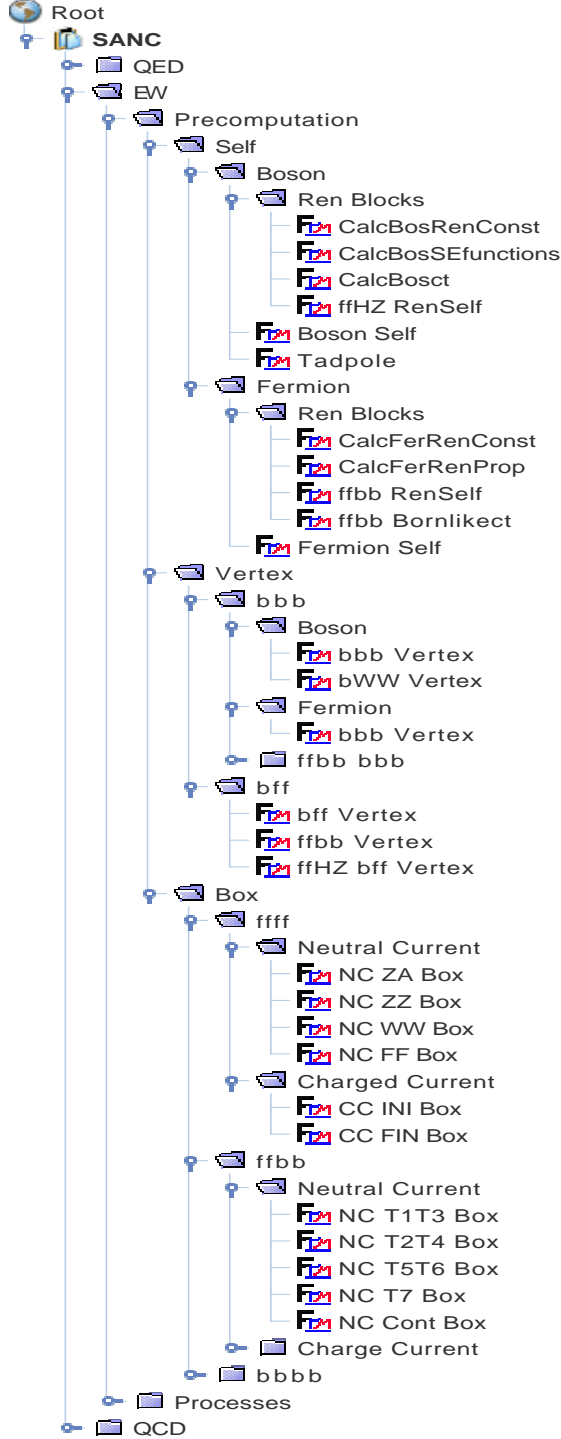


Figure 3: Precomputation in EW part.

It also consists of **Self**, **Vertex** and **Box** sub-items.

Self energies are subdivided into **Boson** and **Fermion** submenus. They are further subdivided into calculation of diagrams themselves: **Boson Self** and **Tadpole** (section 3.2.1) and **Fermion Self** (section 3.2.2). Precomputed and stored one-loop diagrams are used to calculate the corresponding renormalization constants: **CalcBosRenConst** and **CalcFerRenConsts**, which are also stored. They are all used to calculate the ingredients of renormalized bosonic propagators: **CalcBosSEfunctions** and **CalcBosct** and renormalized fermionic propagators **CalcFerRenProp**. The latter is used to calculate the renormalized self energy 4-leg diagram for *ffbb* processes by **ffbb RenSelf**; **ffbb Bornlikeect** computes Born-like counterterms (section 3.2.3).

Vertex consists of 3-boson-leg **bbb** and boson-2-fermion **bff** vertices. Vertices **bbb** contain **Bosonic** and **Fermionic** components and **bbb** vertices for *ffbb* processes (closed here). The former is further subdivided into any neutral leg **bbb Vertex** and in particular any neutral boson to W^+W^- **bWW Vertex** (section 3.3.2). Vertices **bff** are subdivided into any *bff* 3-leg vertices and 4-leg vertices for NC *ffbb* processes (section 3.3.1).

Box is subdivided into three large classes: **ffff**, **ffbb** and **bbbb** each of them is subdivided further into NC and CC boxes. The **ffff** class contains a rich collection of 4-fermion-leg NC and CC boxes, direct and crossed, (section 3.4.1). The **ffbb** family is presented by now by seven topologies of boxes (**NC T1–T7 Box**) appearing in NC *ffbb* processes (section 3.4.2).

The file **NC FF Box** transforms results obtained by **ffff** into the scalar form factors of a *4f* process, while **NC Cont Box** realizes some further manipulations with NC *ffbb* boxes (section 3.4.2).

The files intended for **Charged Current** boxes for *ffbb* processes and for **bbbb** boxes exist but are not added for the time being.

3.2 Self energies

3.2.1 Bosonic self energy

Self energies are the simplest one-loop diagrams. There are three topologies of bosonic self-energy:

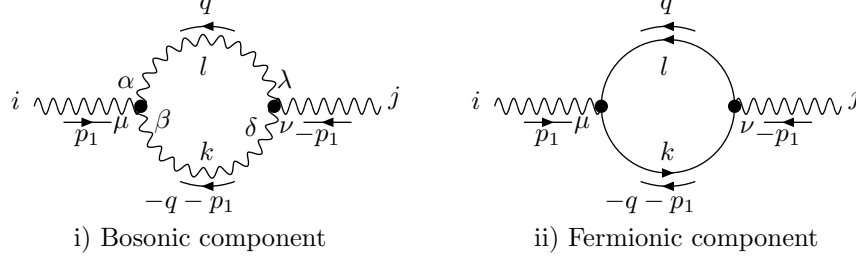


Figure 4: Two point diagrams.

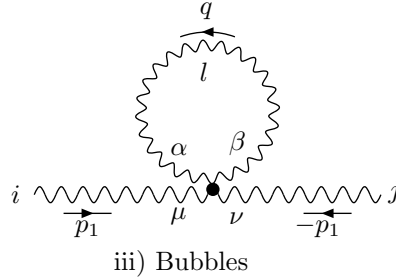


Figure 5: One point bosonic diagrams.

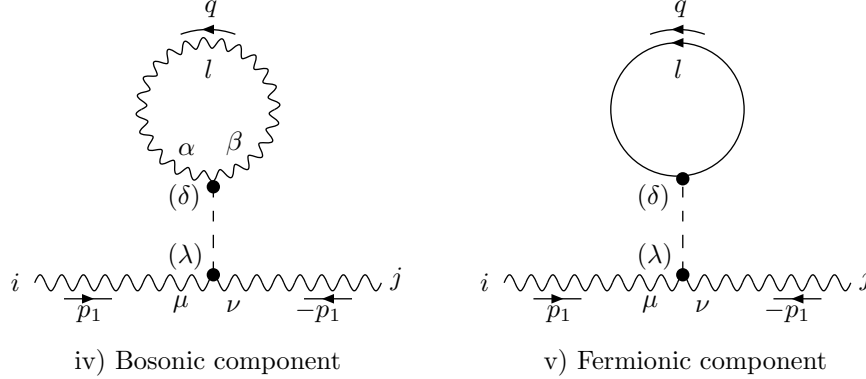


Figure 6: Tadpoles.

For the first and the third topologies it is useful to distinguish *bosonic* and *fermionic* components.

All these diagrams are precomputed and stored in the **BS.sav** file. At user request they may be recomputed by a FORM program accessible via the menu sequence **EW** \rightarrow **Precomputation** \rightarrow **Self** \rightarrow **Boson** \rightarrow **Boson Self**. The five types of self energies are defined in the specific procedure **Diagb(i,j)** (see the definitions of procedure types in the Introduction).

To give an example of what the precomputation really does, we present a simplified version of a very similar module accessible via the menu sequence **QED** \rightarrow **Precomputation** \rightarrow **Self** \rightarrow **Photon** \rightarrow **Photon Self**. It starts with the defining expression **vacpol** for the photonic vacuum polarization, Fig.4 ii) and continues in five steps of calls to the intrinsic procedures (i) **FeynmanRules**, (ii) **Diracizing**, (iii) **GammaTrace**, (iv) **Reduction** and (v) **Scalarizing** described in Section 4.2. After steps 1-4) we show the intermediate results and after step 5) — the final result.

```

#include Declar.h
#call Globals()

g vacpol = -Tr*vert(+1,12,-12,mu,ii)*pr(12,q,ii)
            *vert(-1,12,-12,nu,ii)*pr(12,q+p1,ii)*int;
(i)
#call FeynmanRules(0)

vacpol =
+ den(1,mel,q)*den(1,mel,q+p1)*e^2*qel^2*int*Tr*
(-gd(ii,mu)*gd(ii,q)*gd(ii,nu)*i_*mel-gd(ii,mu)*gd(ii,q)*gd(ii,nu)*gd(ii,q)
-gd(ii,mu)*gd(ii,q)*gd(ii,nu)*gd(ii,p1)+gd(ii,mu)*gd(ii,nu)*mel^2
-gd(ii,mu)*gd(ii,nu)*gd(ii,q)*i_*mel-gd(ii,mu)*gd(ii,nu)*gd(ii,p1)*i_*mel );
(ii)
#call Diracizing(0)

vacpol =
+ den(1,mel,q)*den(1,mel,q+p1)*e^2*qel^2*int*Tr*
(-2*gd(ii,mu)*gd(ii,al1)*qf(al1)*qf(nu)-gd(ii,mu)*gd(ii,al1)*gd(ii,nu)*qf(al1)*i_*mel
-gd(ii,mu)*gd(ii,al1)*gd(ii,nu)*gd(ii,p1)*qf(al1)+gd(ii,mu)*gd(ii,nu)*mel^2
+gd(ii,mu)*gd(ii,nu)*q.q-gd(ii,mu)*gd(ii,nu)*gd(ii,p1)*i_*mel
-gd(ii,mu)*gd(ii,nu)*gd(ii,al1)*qf(al1)*i_*mel );
(iii)
#call GammaTrace(1)

vacpol =
+ den(1,mel,q)*den(1,mel,q+p1)*e^2*qel^2*int*
( 4*d_(mu,nu)*mel^2+4*d_(mu,nu)*q.q+4*d_(mu,nu)*q.p1
-4*qf(mu)*p1(nu)-8*qf(mu)*qf(nu)-4*qf(nu)*p1(mu) );
(iv)
#call Reduction(0)

vacpol =
+ p1(mu)*p1(nu)*e^2*qel^2*
(-8*b21(p1s,1,mel,1,mel)-8*b1(p1s,1,mel,1,mel))
+d_(mu,nu)*e^2*qel^2*
(4*a0(1,mel)-8*b22(p1s,1,mel,1,mel)+4*b1(p1s,1,mel,1,mel)*p1s);
(v)
#call Scalarizing(0)

vacpol =
+ p1(mu)*p1(nu)*e^2*qel^2*
(-4/9-8/3*p1s^-1*mel^2-8/3*a0(1,mel)*p1s^-1+4/3*b0(p1s,1,mel,1,mel)
-8/3*b0(p1s,1,mel,1,mel)*p1s^-1*mel^2 )
+ d_(mu,nu)*e^2*qel^2 *
( 4/9*p1s + 8/3*mel^2 + 8/3*a0(1,mel) - 4/3*b0(p1s,1,mel,1,mel)*p1s
+8/3*b0(p1s,1,mel,1,mel)*mel^2 );

```

We continue describing the structure of the basic program **Boson Self**:

The calculation of all bosonic self-energies (diagram-by-diagram) is done by two calls to specific procedure $\text{CalcBos}(i,j)$, with $\{i = 3, 6, j = i\}$, corresponding to the charged external bosons W^\pm and ϕ^\pm , four calls to $\text{CalcBos}(i,j)$ with $\{i = 1, 2, 4, 5, j = i\}$, corresponding to γ, Z, H and ϕ^0 , and one call to $\text{CalcBos}(i,j)$ with $\{i = 2, j = 1\}$, corresponding to external bosons Z and γ , respectively.

Procedure $\text{CalcBos}(i,j)$ calls specific procedure $\text{Diagb}(i,j)$ and seven *intrinsic procedures*: (i) *FeynmanRules*, (ii) *GammaRight*, (iii) *Diracizing*, (iv) *GammaTrace*, (v) *Reduction*, (vi) *Sing* and (vii) *Scalarizing*. The intrinsic procedures are described in Section 4.2.

At each call to procedure $\text{CalcBos}(i,j)$, the diagrams Figs. 4, 5, 6 are calculated for twelve virtual fermions field indices k, l running over 11, 12 ... 22 (corresponding to $\nu_e, e, u, d, \nu_\mu, \mu, c, s, \nu_\tau, \tau, t$ and b , respectively) and for ten virtual bosons $k, l = 1, 2, \dots, 10$, corresponding to $\gamma, Z, W^\pm, H, \phi^0, \phi^\pm$ and four Faddeev–Popov ghosts X^+, X^-, Y_Z, Y_A , respectively.

The topology of the self-energy diagrams is specified in procedure $\text{Diagb}(i,j)$ in terms of the *vertices* and *propagators* of the diagrams. In the class of diagrams available at present, *vertices* are of two kinds: boson-fermion-fermion (Bff) and three-boson (BBB) vertices. The diagrams are computed in nested loops over all allowed field indices of the virtual particles.

Two more FORM programs are accessible via menu sequences

QED \rightarrow **Precomputation** \rightarrow **Self** \rightarrow **Photon** \rightarrow **Boson Self** \rightarrow **Photon Self** and
EW \rightarrow **Precomputation** \rightarrow **Self** \rightarrow **Boson** \rightarrow **Tadpoles**.

They have very similar structures and compute respectively photonic self energy (vacuum polarization) in the QED tree of SANC and tadpole diagrams separately from self energies. The results are stored in `PSqed.sav` and `TP.sav` files, respectively.

Precomputed bosonic self-energies are used by the other FORM programs which calculate bosonic counterterms

EW \rightarrow **Precomputation** \rightarrow **Self** \rightarrow **Boson** \rightarrow **Ren Blocks** \rightarrow **CalcBosRenConst**

and the photonic counterterm

QED \rightarrow **Precomputation** \rightarrow **Self** \rightarrow **Photon** \rightarrow **CalcPhotRenConst**

in the QED tree; bosonic self energy functions

EW \rightarrow **Precomputation** \rightarrow **Self** \rightarrow **Boson** \rightarrow **Ren Blocks** \rightarrow **CalcBosSEFunctions**,

and the renormalized photonic propagator in the QED branch

QED \rightarrow **Precomputation** \rightarrow **Self** \rightarrow **Photon** \rightarrow **CalcPhotRenProp**.

Their results, in turn, are used by a FORM program which computes *counter term blocks (crosses)*, see Fig. 15 of Ref. [9]. The latter is accessible via the chain

EW \rightarrow **Precomputation** \rightarrow **Self** \rightarrow **Boson** \rightarrow **Ren Blocks** \rightarrow **CalcBosct**.

3.2.2 Fermionic self energy

There are two topologies of fermion self energy diagrams (two point diagrams Fig. 7 and tadpoles Fig. 8).

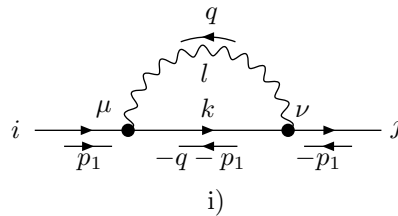


Figure 7: Two point diagrams.

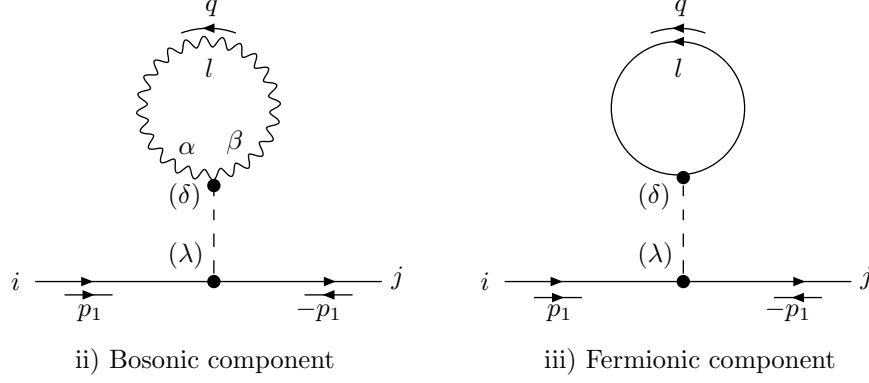


Figure 8: Tadpoles.

These diagrams are precomputed and stored in the `FS.sav` file. They may be recomputed by a FORM program accessible via the menu sequence

EW → Precomputation → Self → Fermion → Fermion Self.

The three types of diagrams are defined in the specific procedure `Diagf(i,j)`.

Structure of the program **Fermion Self**:

The calculation is done by 12 calls to specific procedure `CalcFer(i,j)`, with $i = j = 11, 12 \dots, 22$, corresponding to all fermions of four generations, respectively.

Procedure `CalcFer(i,i)` calls specific procedure `Diagf(i,j)` and seven intrinsic procedures (i) Feynman-Rules, (ii) `GammaRight`, (iii) `Diracizing`, (iv) `GammaTrace`, (v) `Reduction`, (vi) `Sing` and (vii) `Scalarizing`, see Section 4.2.

At each call to procedure `CalcFer(i,i)`, the diagrams Figs. 7 and 8 are calculated for twelve virtual fermions $i = 11, 12 \dots, 22$ and only six virtual bosons $l = 1, 2, \dots, 6$, corresponding to $\gamma, Z, W^\pm, h, \phi^0$ and ϕ^\pm , respectively, since Faddeev–Popov ghosts do not contribute here.

The topology of the self-energy diagrams is specified in procedure `Diagf(i,j)` in terms of the vertices and propagators of the diagrams as well as *sign* and *combinatorial* factors (`sign('l')` and `cft('l')`).

There is one more FORM program, accessible via the menu sequence

QED → Precomputation → Self → Lepton → Lepton Self

whose structure is very similar to program `Fermion Self`. It computes the leptonic self energy in the QED tree of `SANC`. The results are stored in `LSqed.sav` file. Precomputed fermionic self-energies are used by FORM programs which calculate fermionic counterterms

EW → Precomputation → Self → Fermion → Ren Blocks → CalcFerRenConst

and leptonic counterterms

QED → Precomputation → Self → Lepton → CalcLepRenConst.

Both fermionic self-energy diagrams and fermionic counterterms are used by FORM programs which compute the renormalized fermionic (leptonic in the QED branch) propagators

EW → Precomputation → Self → Fermion → Ren Blocks → CalcFerRenProp and

QED → Precomputation → Self → Lepton → CalcLepRenProp, respectively.

In the FORM code `CalcLepRenProp` we show the main steps of the calculations. The two latter codes end up demonstrating the vanishing of the renormalized propagator on the corresponding fermionic mass shell, as is required by the on-mass-shell (OMS) renormalization scheme, see Section 2.2 of [9].

3.2.3 Fermionic self energy for $ffbb$ processes

Moving to precomputation of the building blocks for $ffbb$ processes, we change our conventions. Now any object: self energy, vertex and box are considered to be 4-legs, rather than 2-, 3- and 4-legs respectively, as we did before. The main motivation for this change is our observation that vertices with off-shell fermions are inconvenient to treat and the resulting expressions are more compact if we consider 4-legs on-mass-shell building blocks instead of 3-legs off-shell. Accepting this convention for vertices, it is natural to treat self-energies also like 4-leg objects shown in Fig. 9:

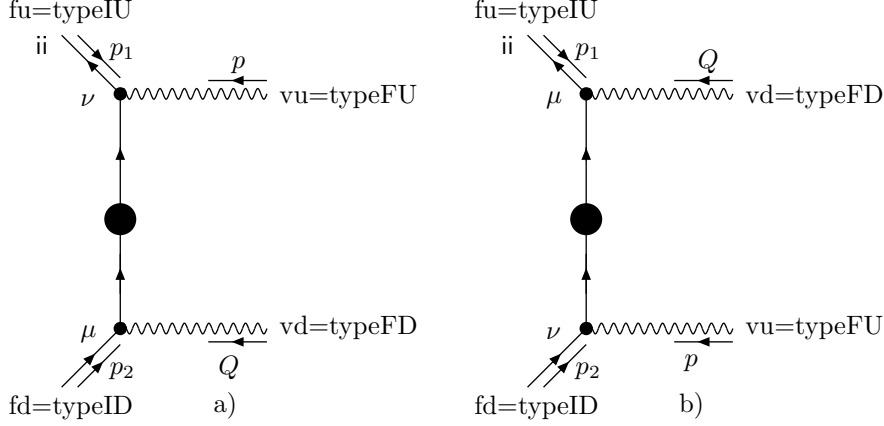


Figure 9: Self energy $ffbb$ diagrams.

Here the blob at the fermion propagator denotes the sum of all self-energy diagrams described in Section 3.2.2. These self energies are precomputed by a FORM program accessible via the menu sequence **EW** \rightarrow **Precomputation** \rightarrow **Self** \rightarrow **Fermion** \rightarrow **Ren Blocks** \rightarrow **ffbb RenSelf**.

The required CPU time is still very short, and at user request they may be re-computed. The two types of self energies are defined in the specific procedures `CalcFerSEt(fu,fd,vd,vu)` and `CalcFerSEu(fu,fd,vu,vd)`, which use renormalized fermionic propagators precomputed by **CalcFerRenProp**. Note that the labels 't' and 'u' are associated with the Mandelstam variables t, u , see Section 2.4.

Both t and u channel procedures call intrinsic procedures `FeynmanRules`, `GammaRight` and `p2l` where the latter, together with several `id`'s in between, performs obvious identities and change of variables.

Computed diagrams `FSEt'fu'fd'vd'vu'jl'k1'` and `FSEu'fu'fd'vu'vd'jl'k1'` are stored in the file `ffbbSelfxi'xi'fu'fd'vu'vd'.sav`, where the predefined parameter 'xi' has the following meaning:

```
#define xi "0" / * .eq.0 to test gauge invariance / * .eq.1 to work in xi=1 gauge
```

This option is introduced mostly to save CPU time since calculation in the $\xi=1$ gauge are much faster than in the R_ξ gauge. However, it is always appealing to see the explicit cancellation of gauge parameters. That is why we try to maintain option `xi "0"` as long as possible even though in some cases it is extremely time consuming.

There is a similar FORM program in the QED part, accessible via the menu sequence **QED** \rightarrow **Precomputation** \rightarrow **Self** \rightarrow **Lepton** \rightarrow **Ren Blocks** \rightarrow **IIAA RenSelf**.

Furthermore, the code, accessible via menu sequence:

EW \rightarrow **Precomputation** \rightarrow **Self** \rightarrow **Fermion** \rightarrow **Ren Blocks** \rightarrow **ffbb Bornlikect**

computes contributions from four diagrams similar to Fig. 9, in which the self energy blob at the fermion propagator is replaced by counterterm 'crosses' (one for each of the four diagrams at each vertex with indices μ and ν , similar to Fig. 12). The result is stored in the file `ffbbBornlikectxi'xi'fu'fd'vu'vd'.sav`.

The file from **QED** \rightarrow **Precomputation** \rightarrow **Self** \rightarrow **Lepton** \rightarrow **Ren Blocks** \rightarrow **ffAA Bornlikect** does the same job in the QED part.

3.3 One-loop vertices

The current SANC version has all bff and bbb 3-leg SM vertices.

3.3.1 bff vertices

There are two topologies of bff vertices: FBF and BFB:

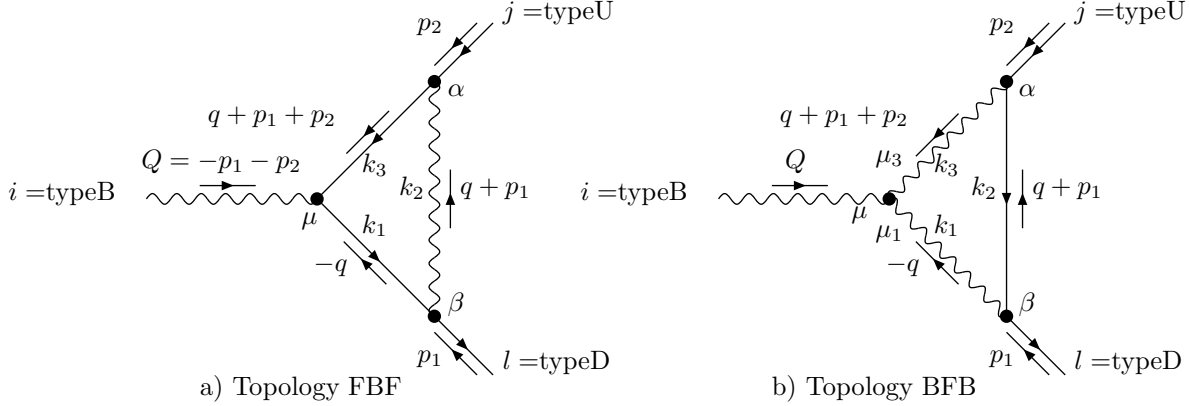


Figure 10: bff vertices.

These vertex diagrams are precomputed by a FORM program accessible via menu sequence

EW \rightarrow Precomputation \rightarrow Vertex \rightarrow bff \rightarrow bff Vertex.

At user request they may be recomputed. The two types of vertices are defined in the specific procedures $FBF(i,j,l)$ and $BFB(i,j,l)$, where the topologies of all vertices of the type of Fig. 10 are specified in nested loops over all allowed field indices of the virtual particles.

Structure of program **bff Vertex**

The calculation is done by a single call to specific procedure $CalcVertex('typeB', 'typeU', 'typeD')$, followed by a call to intrinsic procedure $p2D$.

The arguments `typeB`, `typeU`, and `typeD` are the field indices of the external particles, set in the command that starts this program: `typeB` is the incoming boson, `typeU` is the antifermion with incoming 4-momentum p_2 , and `typeD` is the fermion with incoming 4-momentum p_1 . For instance, to calculate the vertex for $Z \rightarrow u\bar{u}$ decay, `typeB`, `typeU`, and `typeD` are set equal to 2, 13, 13, respectively. The results are stored in files `V'typeB'typeU'typeD.sav`.

Procedure $CalcVertex(i,j,l)$ calls specific procedures $FBF(i,j,l)$ and $BFB(i,j,l)$ and the intrinsic procedures in the following sequence: `FeynmanRules`, `GammaRight`, `Diracizing`¹, `Reduction`, `Diracizing`, `Pulling`, `Diraceq`, `Sing`, `Scalarizing`, `2Qs`, `Massshell` and `Symmetrize`. The intrinsic procedures are described in Section 4.2.

In the QED tree there is a similar entry

QED \rightarrow Precomputation \rightarrow Vertex \rightarrow Aff \rightarrow Aff Vertex,

which computes $\gamma l\bar{l}$ vertices for a lepton of a kind $j = \text{typeU} = 12, 16, 20$. These vertices are defined in the specific procedure $DiagVert(j)$. The results are stored in files `Vqed'typeU.sav`.

¹For Wff vertices, this procedure is called exceptionally in the so-called *special use mode*, see Section 4.2. This is due to a delicate treatment of the auxiliary Passarino-Veltman functions originating from a double pole $1/(p^2)^2$ in the photonic propagator in the R_ξ gauge.

3.3.2 bbb vertices

The *bosonic* component of three-boson vertices has four topologies shown in the following diagrams:

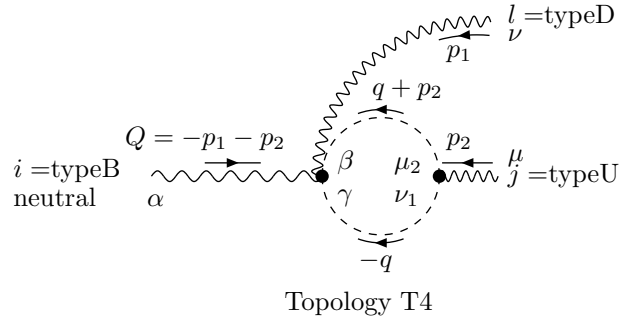
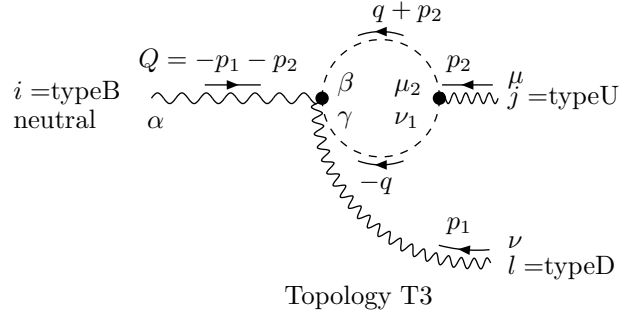
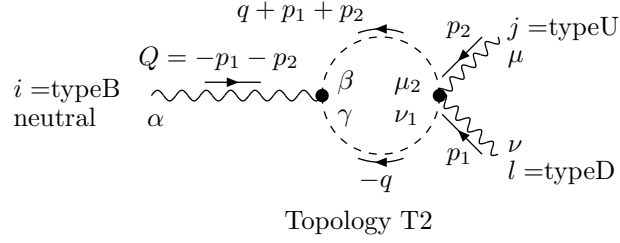
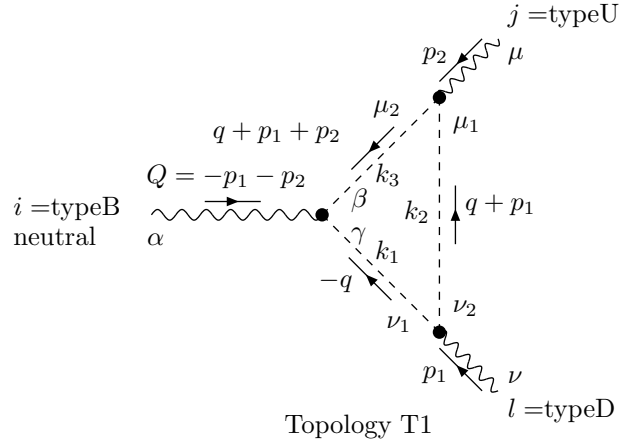


Figure 11: Four topologies for three-boson vertices.

These vertex diagrams are precomputed by a FORM program accessible through the chain of clicks **EW** → **Precomputation** → **Vertex** → **bbb** → **Boson** → **bvv Vertex**.

They also may be recomputed at user request. The four topologies are defined in the specific procedures TribosVertT1(i,l,j).

Structure of program **bvv Vertex**

The calculation is done by a single call to specific procedure CalcTribosVertT14('typeB','typeD','typeU') which calls first of all four topologies in Figs. 11 defined in specific procedures TribosVertTk(i,l,j), with $k = 1, 2, 3, 4$.

Just after that four specific procedures CITribosVertTk(i,l,j) perform *clusterizing* of the computed diagrams. One should note that *clusters* have different meanings in SANC. Here clusterizing means nothing but summation over all virtual field indices, resulting in the dependence of cluster names only on external field indices.

After clusterizing, the usual calls of the intrinsic procedures follow: FeynmanRules, 2Qs, Reduction, 2Qs, Sing and Scalarizing.

The *fermionic* component of three-boson vertices has only one topology T1. The diagrams are defined in the specific procedure TribosVertf(i,l,j).

Structure of program **Fermion** → **bbb Vertex**

The calculation is done by a single call to specific procedure CalcTribosVert('typeB','typeD','typeU') which at first calls the topology defined in the specific procedure TribosVertf(i,l,j). Next, specific procedure CIT1fer(i,l,j) performs *clusterizing*.

The calculation of the cluster is followed by calls of the intrinsic procedures: FeynmanRules, Gamma-Left, Diracizing, GammaTrace, Reduction, Scalarizing, Sing, Scalprod and DivisionGramDet.

One may access a similar FORM code to precompute the HWW, ZWW and AWW vertices via sequence **EW** → **Precomputation** → **Vertex** → **bbb** → **Boson** → **bWW Vertex**.

3.3.3 Vertices for *ffbb* processes

There are four blocks of vertices met in *ffbb* processes where only diagrams with fermion exchange contribute at the Born level (we have also *ffZH* process where there is the Born diagram with boson exchange, so-called Higgsstrahlung, but this process is not added to SANC v.1.00):

The four building blocks are precomputed by a FORM program accessible via menu sequence:

EW → **Precomputation** → **Vertex** → **bff** → **ffbb Vertex**.

Structure of program **ffbb Vertex**

The calculation is done by $2 \otimes 3$ calls to the following specific procedures:

CalcVert('typeFU','typeID','typeIU',mu)	— computes vertex blob with index μ ;
CalcVertmut('typeIU','typeID','typeFD','typeFU',mu)	— computes diagram b);
CalcVertmuu('typeIU','typeID','typeFU','typeFD',mu)	— computes diagram c);
CalcVert('typeFD','typeID','typeIU',nu)	— computes vertex blob with index ν ;
CalcVertnut('typeIU','typeID','typeFD','typeFU',nu)	— computes diagram d);
CalcVertnuu('typeIU','typeID','typeFU','typeFD',nu)	— computes diagram a).

The procedure CalcVert recomputes *bff* vertices for given set 'typeFU','typeID','typeIU' and creates expressions vbf'vu''fd''fu''mu''k1''k2''k3' and vbfb'vu''fd''fu''mu''k1''k2''k3' similar to those described in Section 3.3.1, but not applying intrinsic procedure Masshell since in the case under consideration one of fermions is off-shell. The four procedures CalcVertmut, CalcVertmuu, CalcVertnut and CalcVertnuu have very similar structures.

In each of four procedures the intrinsic procedures FeynmanRules, GammaRight, bplidentities, p2m, p2l and p2p are called. Next follows an important shift of the virtual fermion 4-momenta to 'real' four

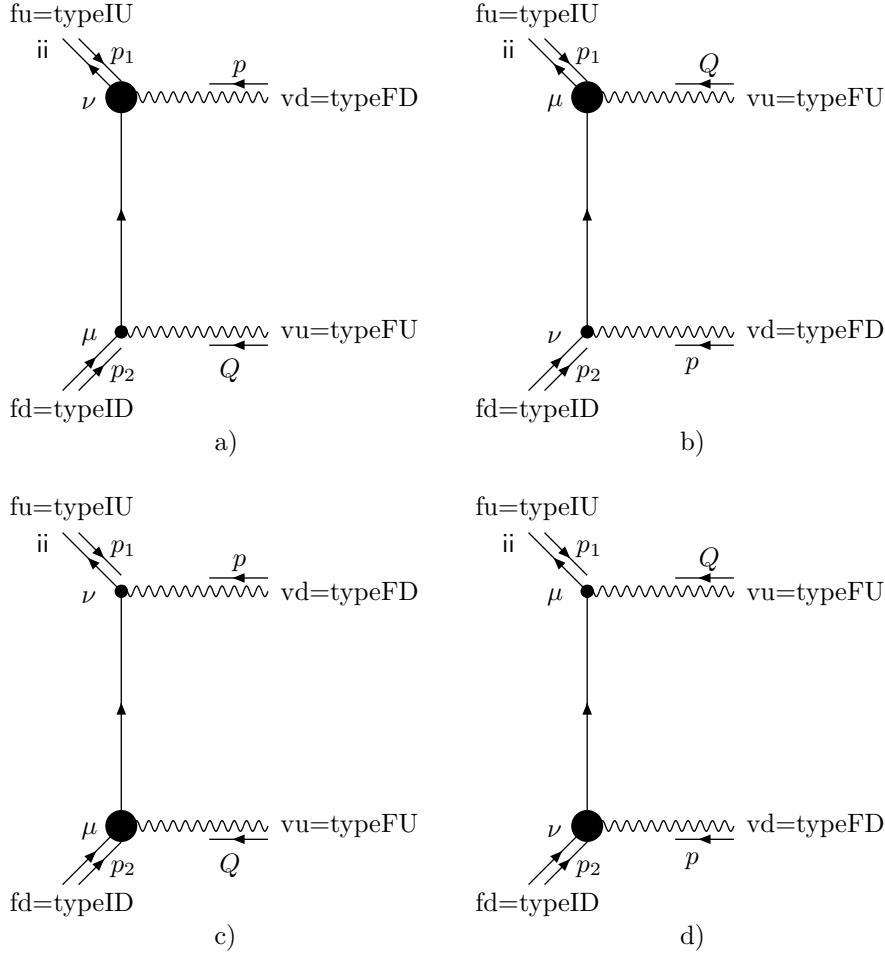


Figure 12: Four ffb vertex diagrams.

momenta p_1, p_2, p, Q , and finally `ExtMomentumWI` is applied.

All the building blocks are clusterized by summation over virtual momenta in vertex loops (see discussion of clusterization in Section 3.4.2.).

Besides `xi` there are three more internally defined options: `on` (see Section 3.4.2 for more discussion about option `on`) and `mf`, `mp`, of which the latter two allow to neglect fermion masses.

```
#define on "1"
* .eq.0 photons are off mass-shell; .eq.1 photons are on mass-shell
#define mf "0"
* .eq.0 fermion mass, pm('typeID')=0; .eq.1 it is not neglected
#define mp "0"
* .eq.0 partner mass, pm('typeIDp')=0; .eq.1 it is not neglected
```

The result of this calculation is stored in the file

`ffbbVertxi'xi'on'on'mf'mf'mp'mp' 'typeIU''typeID''typeFU''typeFD'.sav.`

3.4 One-loop boxes

Approaching the description of precomputation of boxes, one should note that the world of boxes is much more rich and complex compared to self-energies and vertices. If for the latter case we still could profess the idea of allowing recomputation of all one-loop vertices needed for the process under consideration, then in the case of boxes we must change our strategy if the user wants to carry out some recomputation.

For boxes, the idea of precomputation becomes vitally important for realization of SANC project. As will be explained below, calculation of some boxes for some particular processes takes so much time that an external user should refrain from repeating precomputation. Furthermore, the richness of boxes requires more classification. Depending on the type of external lines (fermion or boson), we will distinguish three large classes of boxes: ffff, ffbb and bbbb.

3.4.1 Boxes for $ffff$ processes

The ffff boxes, which are met in the description of $4f$ processes, are of two topologies, *direct* and *crossed*, and are characterized by two fermionic currents ii and jj , coupled by two bosons with field indices $k1$ and $k3$; see Fig. 13 showing all the field indices (for external and virtual fields), types of external fermions $typeXX$, Lorentz indices and momentum flows for the direct and crossed topologies.

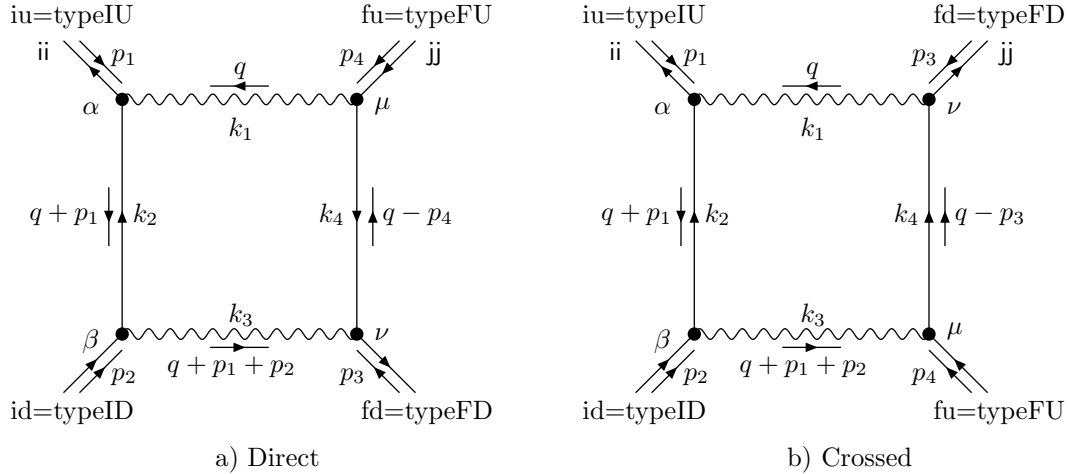


Figure 13: Direct and crossed boxes for $ffff$ processes.

These diagrams describe both *neutral current* (NC) and *charged current* (CC) boxes both for $1 \rightarrow 3$ decays and $2 \rightarrow 2$ reactions in any channel (s, t, u) . In the general case, virtual boson field indices run from 1 to 6, and virtual fermion indices run over doublets $\{typeID, typeIDp\}$ and $\{typeFU, typeFUp\}$, where $typeIDp$ and $typeFUp$ are isospin partners of $typeID$ and $typeFU$, respectively.

The calculation of direct and crossed boxes is realized in two specific procedures `direct(iu,id,fu,fd)` and `crossed(iu,id,fu,fd)` in nested loops over all allowed field indices of the virtual particles.

Such a realization may apparently take into account all the external fermion masses. However, in practical applications we usually treat fermion masses of one of two currents, ii or jj , as being massless, which is true for the processes of the kind $f_1 + f_1 + f + f \rightarrow 0$, upon which we concentrate. Here f_1 denotes a massless first generation fermion or any neutrino.

Various FORM codes computing these boxes are accessible via chains of clicks

EW → Box → ffff → Neutral Current → NC ZZ(ZA,WW) Box and

EW → Box → ffff → Charged Current → CC INI(FIN) Box.

Here INI(FIN) means which of the masses, initial fermions *ii* or final fermions *jj* are kept non-zero. All the codes have very similar structures with minor modifications. The calculation is done by a single call to specific procedure `CalcBoxNC('typeU','typeD','typeFU','typeFD')` which calls first the two specific procedures — `direct(iu,id,fu,fd)` and `crossed(iu,id,fu,fd)`. In these procedures all the box diagrams are defined in terms of vertices, propagators and external spinors `tlo(p1)`, `tro(p2)`, `tle(p3)` and `tre(p4)`.

The subsequent calculations are very similar for all 4f-boxes, both NC and CC.

In the beginning of each NC(CC) XX Box program, described in this Section, there is an internal definition `#define xi "0"` which chooses among two internal options with an obvious meaning described in Section 3.2.3.

Note, that for 4f boxes we gain only little CPU time choosing `xi "1"` option, since action of `BoxPre-reductionNC(CC)` results in nearly complete cancellation of ξ already before `Scalarizing`. For example, the program NC ZA Box needs about 3 minutes CPU time at a 1.6 GHz computer for both options. A similar picture is valid also for the program CC FIN Box.

Actually, 4f-boxes are the last precomputation programs which still may be recomputed at user request. However, we do not recommended to recompute them, because 3 min is already a noticeable time.

The results of calculations of NC boxes are stored in the files `ffffZZxi'xi''typeU''typeD''typeFU''typeFD'.sav` and `ffffZAXi'xi''typeU''typeD''typeFU''typeFD'.sav` and are loaded by a FORM program

EW → Box → ffff → Neutral Current → NC FF Box

which constructs box form factors stored in the files `ffffNCFf'typeU''typeD''typeFU''typeFD'.sav`. This special FORM program will be described elsewhere.

3.4.2 Boxes for *fbb* processes

There are seven topologies of boxes which are met in the description of 2f2b processes. Their enumeration is borrowed from Ref. [1]. All these boxes have apparently only one fermionic current conventionally marked by the current index *ii* but different numbers of internal bosonic lines.

Topologies T2, T4

We begin with the simplest case of topologies having only one virtual bosonic line, see Fig. 14 showing all the field, type and Lorentz indices and momentum flows. These two topologies are actually of the type of direct and crossed ones considered in the previous section. However, their structure is quite different.

These diagrams also describe both NC and CC boxes in any channel (*s,t,u*), both decays and reactions. The virtual boson field indices run from 1 to 6, and virtual fermion indices run over doublets `{typeID,typeIDp}`, where `typeIDp` is the isospin partner of `typeID`. It is foreseen to cover CC processes in the future; currently we have only NC processes.

The calculation of T2 and T4 topologies is realized in two specific procedures `boxT2(fu,fd,vd,vu)` and `boxT4(fu,fd,vu,vd)` in nested loops over all allowed field indices of the virtual particles. Contrary to the 4f-case, we do take into account the external fermion masses.

The calculation starts by two calls to specific procedures `CalcBoxT2('typeU','typeD','typeFD','typeFU')` and `CalcBoxT4('typeU','typeD','typeFU','typeFD')` which call two specific procedures shown above.

Then, for each topology, the calculation continues by clustering boxes calling the procedure `ClusterboxT2(4)('fu','fd','vd','vu')` which creates four clusters, `Cl'k'T2(4)'fu''fd''vd''vu'` for *k*=1,4, depending on ξ_A , ξ_Z , ξ_W , and independent of any ξ , respectively. Next follow calls to the intrinsic procedures `FeynmanRules`, `GammaRight`, `Diracizing`, `Diraceq`, `Reduction`, `Pulling`, `Diraceq`, `PullingOrder`, `Scalprod`, `Sing`, `ExtMomentumWI` described in Section 4.2.

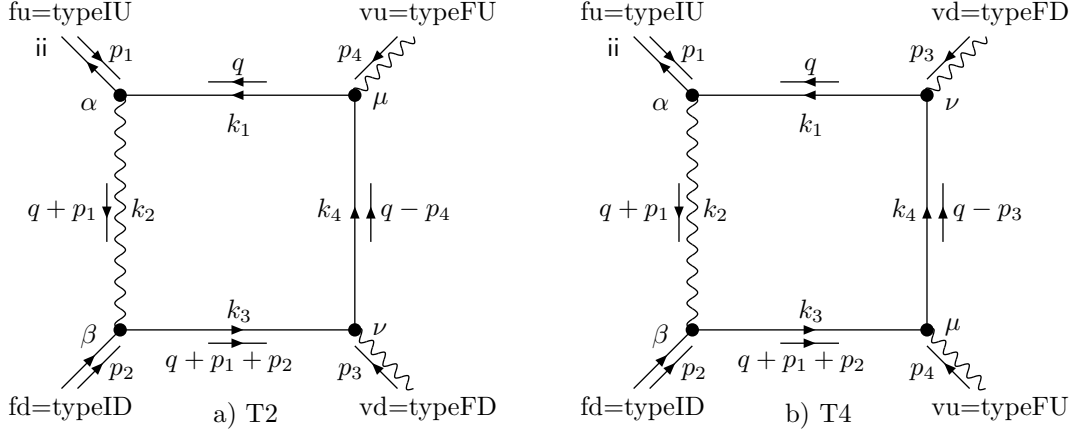


Figure 14: Boxes for $ffbb$ processes, topologies T2 and T4.

Then follows a do-loop over k making separate scalarizations of four clusters inside which six more intrinsic procedures are called: `Scalarizingdp`, `Scalarizing`, `DivisionGramDet`, `bplidentities`, `p2m`, `p2p`.

In the beginning of the program there are four usual definitions:

```
#define xi "0" / #define on "0" / #define mf "1" / #define mp "1".
```

the meaning of three of which was explained in the previous sections.

Note that for the $2f2b$ processes where one (or two) bosons are photons one may, of course, choose on "1" which greatly saves CPU time (see tables of CPU time below in this section). Option on "0" is basically foreseen for $2 \rightarrow 3$ processes where these $2f2b$ boxes with off shell boson(s) are building blocks.

The results of calculations of these boxes are stored in the files `ffbbT2xi'xi'on'on'mf'mf'mp'mp'fu'fd'vd'vu'.sav` and `ffbbT4xi'xi'on'on'mf'mf'mp'mp'fu'fd'vu'vd'.sav`.

The calculation of $2f2b$ boxes takes a lot of CPU time. The NC T2T4 Box is the fastest, but even this program should not be recomputed by users. The other $ffbb$ box topologies, except T7, take much more CPU time.

In conclusion of this section we present an instructive example of how much CPU time is needed to compute T2+T4 topologies for the $d\bar{d} \rightarrow \gamma\gamma$ process at a 3 GHz PC running Linux:

```
xi "0", on "0", mf "1", mp "0" — 5 hours,
xi "0", on "1", mf "1", mp "1" — 70 minutes,
xi "1", on "1", mf "1", mp "1" — 60 minutes.
```

This is why a recomputation of these boxes is not allowed.

Topologies T1, T3

We jump now to the most complex case of topologies having three internal bosonic lines, see Fig. 15 showing all the field, type and Lorentz indices and momentum flows. These two topologies are also of the type of direct and crossed ones, however their structure is much more complex than anything considered so far.

The paragraph after Fig. 14 applies also in this case.

The calculation of T1 and T3 topologies is realized in two specific procedures `boxT1(fu,fd,vd,vu)` and `boxT3(fu,fd,vu,vd)` in nested loops over all allowed field indices of the virtual particles. As before, we take into account the external fermion masses.

So far we have considered $2f2b$ processes for the case when one of the bosons is a photon. In such a case the internal bosons must be charged (with field indices ± 3 and ± 6).

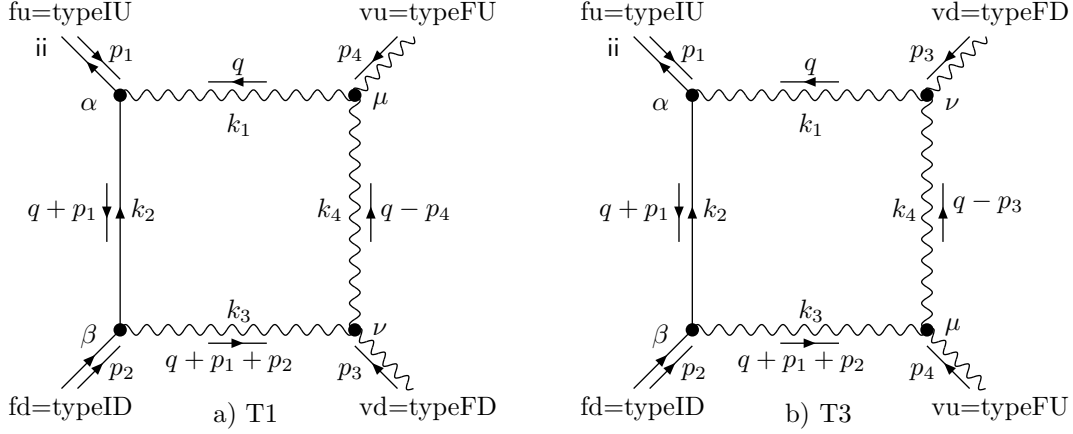


Figure 15: Boxes for $ffbb$ processes, topologies T1 and T3.

The calculation starts by two calls to specific procedures `CalcBoxT1('typeIU','typeID','typeFD','typeFU')` and `CalcBoxT3('typeIU','typeID','typeFU','typeFD')` which call the two specific procedures mentioned above.

Then, for each topology, the calculation continues by calling the procedure `ClusterboxT1(3)(fu,fd,vd,vu)` which creates in this case only two clusters, `Cl'k'T1(3)'fu'fd''vd''vu'` for $k=2,3$, where $k=2$ collects all neutral virtual bosons and $k=3$ all charged bosons. Next follow standard calls to the intrinsic procedures `FeynmanRules`, `GammaRight`, `Diracizing`, `Diraceq`, `Reduction`, `Pulling`, `Diraceq`, `PullingOrder`, `Scalprod`, `Sing`, `ExtMomentumWI` described in Section 4.2.

Then follows a call to the intrinsic procedure `ScalarizingProj` which scalarizes two clusters, $k=2,3$, splitting them first into as many Dirac–Lorentz structures as it has. This is done in order to avoid limitations of FORM v3.0 which cannot handle internal files of length greater than 1.6 Gb or so. This might be circumvented by switching to FORM v3.1, however, we did not manage to switch to this version so far.

Inside itself procedure `ScalarizingProj` creates many intermediate expressions to which intrinsic procedures `Scalarizing`, `DivisionGramDet`, `p2m` are applied. At the end, `ScalarizingProj` collects these pieces together again.

The intrinsic procedure `p2p` is called at the end.

The results of calculations of boxes of T1 and T3 topologies are stored in the files `ffbb'k'T1xi'xi'on'on'mf'mf'mp'mp''fu''fd''vd''vu'.sav` and `ffbb'k'T3xi'xi'on'on'mf'mf'mp'mp''fu''fd''vu''vd'.sav`.

The label 'k' stands for two clusters: $= 2$ with all *neutral* virtual bosons, and $= 3$ with all charged virtual bosons 'k1','k3','k4'.

In the beginning of the program there are four usual definitions:

```
#define xi "0" / #define on "0" / #define mf "1" / #define mp "1"
```

having the same meaning as explained in the previous section.

A table of CPU times for the $d\bar{d} \rightarrow \gamma\gamma$ boxes of topologies T1+T3 looks as follows:

xi "0", on "0", mf "1", mp "0" — 90 hours,

xi "0", on "1", mf "1", mp "1" — 7 hours,

xi "1", on "1", mf "1", mp "1" — 14 minutes.

Of course, a recomputation of these boxes is not allowed.

Topologies T5, T6

Now we switch to the intermediate case of topologies having two internal bosonic lines, see Fig. 16 showing all the field, type and Lorentz indices and momentum flows. These two topologies are *not* the usual pair of direct and crossed ones. Note that they are both drawn as two different direct boxes.

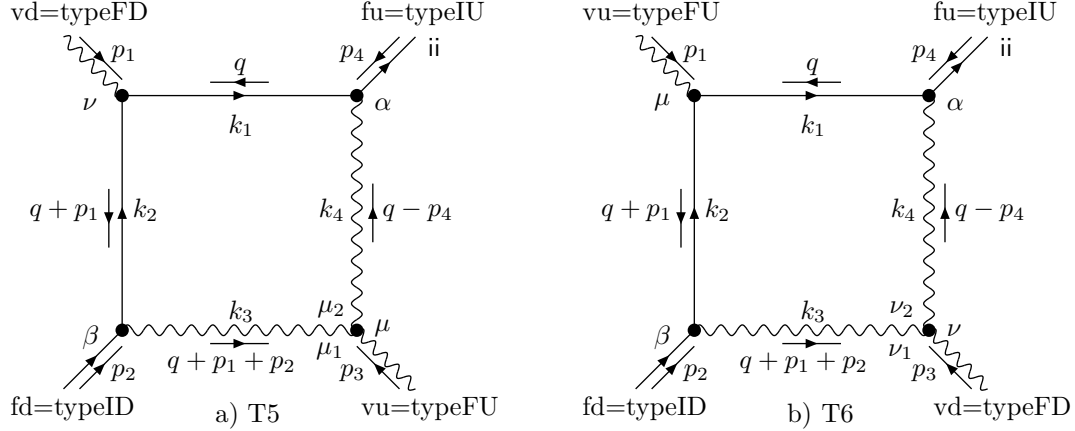


Figure 16: Boxes for ffb processes, topologies T5 and T6.

The paragraph after Fig. 14 is applicable here too. For these topologies, contrary to all previous cases, the leptonic current flows through the diagram: from lower-left (p_2) to upper-right corner (p_4), rather than from lower-left (p_2) to upper-left corner (p_1). This forces us to introduce the notion of *in the sense of Reduction*, i.e. to perform the calculation of a diagram denoting momentum flows as is suitable for Reduction and at the end come back to the *Real* notation for external momenta and Mandelstam invariants. This is why the corresponding procedure is called `isoR2Real`, see Section 4.2.

The calculation of T5 and T6 topologies is realized in two specific procedures `boxT5(vd,fd,vu,fu)` and `boxT6(vu,fd,vd,fu)` in nested loops over all allowed field indices of the virtual particles.

Even though we consider the processes with a photon, for this case internal bosons can be charged or neutral if the photon is coupled to the fermion line. The virtual fermion index runs over a doublet.

The calculation starts by several calls to specific procedure `CalcBoxT5('typeFD','typeID','typeFU','typeIU',k3min,k3max,k4min,k4max)` and by a single call to `CalcBoxT6('typeFU','typeID','typeFD','typeIU',k3min,k3max,k4min,k4max)`. They, in turn, call the two specific procedures shown above.

Such an asymmetry is due to the fact that we assume 'typeFD' to be a photon, and therefore the virtual bosons in diagram T6 must be charged: $k3min=3, k3max=6, k4min=3, k4max=6$. Note, that $k3=\{k3min,k3max\}$ and $k4=\{k4min,k4max\}$.

For diagrams with two virtual bosons the clustering is performed in the following way:

- Cluster 22, $k3=\{2,5\}, k4=\{2,5\}$
- Cluster 33, $k3=\{3,6\}, k4=\{3,6\}$
- Cluster 42, $k3=\{4,4\}, k4=\{2,5\}$
- Cluster 24, $k3=\{2,5\}, k4=\{4,4\}$
- Cluster 44, $k3=\{4,4\}, k4=\{4,4\}$

Then the calculation continues for each topology by calls to the intrinsic procedures `FeynmanRules`, `GammaRight`, `Diracizing`, `Reduction`, `Pulling`, `Diraceq`, `PullingOrder`, `Scalprod`, `Sing`, `ExtMomentumWI` and then to `ScalarizingProj` as described in the previous section.

The intrinsic procedures `p2p` and `isoR2Real` are called at the end.

The results of calculations of boxes of T5 and T6 topologies are stored in the files `ffbb'k3min''k4min'T5xi'xi'on'on'mp'mp''vd''fd''vu''fu'.sav` and `ffbb'k3min''k4min'T6xi'xi'on'on'mp'mp''vu''fd''vd''fu'.sav`.

In the beginning of the program there are usual definitions:

```
#define xi "0" / #define on "0" / #define mf "1" / #define mp "1"
```

A table of CPU times for the $d\bar{d} \rightarrow \gamma\gamma$ boxes of topologies T5+T6 reads:

```
xi "0", on "0", mf "1", mp "0" — 32 hours,  
xi "0", on "1", mf "1", mp "1" — 4.5 hours,  
xi "1", on "1", mf "1", mp "1" — 19 minutes.
```

A recomputation of these boxes is not allowed either.

Topology T7

Topology T7 also has two internal bosonic lines, see Fig. 17, however it is rather a pinch of topologies T1 and T4 (bosonic line with field index k_4 is pinched out).

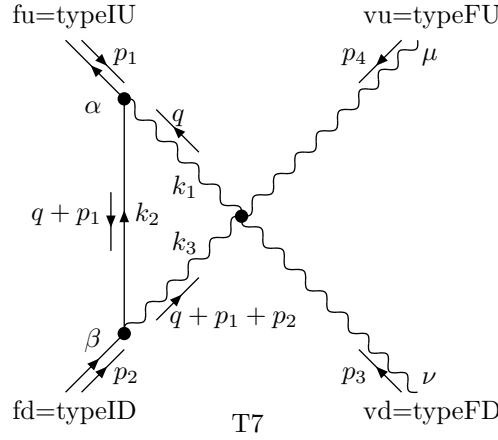


Figure 17: Boxes for $f\bar{f}b\bar{b}$ processes, topology T7.

The calculation of the T7 topology is realized in the specific procedure `boxT7(fu,fd,vd,vu)` in nested loops over field indices. If there is only one photon in the final state, the virtual bosons must be charged. This is why there is only one cluster in this case.

This is a vertex-like diagram and for this reason it is much simpler than all the others.

The calculation starts by a single call to specific procedure `CalcBoxT7('typeIU','typeID','typeFD','typeFU')` which calls the procedure `boxT7` shown above.

The calculation continues by calls to the intrinsic procedures `FeynmanRules`, `GammaRight`, `Diracizing`, `Diraceq`, `Reduction`, `Pulling`, `Diraceq`, `Scalprod`, `Sing`, `ExtMomentumWI`, `Scalarizing`, `p2m`, `DivisionGramDet`.

The results are stored in the file `ffbbT7xi'xi'on'on'mp'mp''fu''fd''vd''vu'.sav`.

In the beginning of the program there are four usual definitions:

```
#define xi "0" / #define on "0" / #define mf "1" / #define mp "1".
```

The topology T7 needs only a few seconds of CPU time.

4 SANC Procedures

4.1 Introduction

At Level 1 the SANC database contains FORM *programs* and *procedures*. All FORM programs are accessible for the user via a sequence of clicks on SANC tree, when we reach a file and open it. The situation is very different for the procedures which are of three kinds: *specific*, *special* and *intrinsic*.

A procedure is called specific if it is used only in one particular program. Normally, specific procedures are included in the corresponding FORM program body and are also open for the user. Moreover, they are very easy to read and describe.

Special procedures are usually used by only a limited number of FORM programs and, similar to specific procedures, they do a job which is relevant for these programs only. However, contrary to specific procedures we do not open them for the users, since their content is not so transparent to be read and described. It is envisaged to upgrade special procedures to the level of intrinsic procedures in future versions of SANC.

Intrinsic procedures are used by many FORM programs and should be easily used in any new program. Their functions are totally determined by the list of their arguments which are of two types: genuine arguments (FORM variables), denoted below as **AVALUE**, and *options*, usually integer numbers, denoted as **IVALUE**, which are used as switches governing calculation flow inside the procedure. Sometimes an **IVALUE** (see below) stands for a *special use*, i.e. a special flow inside an intrinsic procedure.

4.2 Intrinsic procedures

Below we give a list of intrinsic procedures which are mostly met in the **Precomputation** trees of SANC. In this list, which is not complete by far, the procedures are presented in alphabetic order, and the ‘treatment’ of their options and arguments is explained.

a2b : replaces symbol “a” to symbol “b”. Possible arguments: $s_w \rightarrow c_w$, $M_w \rightarrow M_z$, $\gamma_6 \rightarrow \gamma_5$, $\gamma_7 \rightarrow \gamma_5$, $\sigma_i \rightarrow \sigma_j$, $\delta_i \rightarrow \delta_j$ etc. and *vice versa*.

AVALUE = (s_w, c_w) , for example.

bpIdentities : applies identities to the so-called auxiliary Passarino–Veltman functions (bp0= b_0 and bp1= b_1 [1]), attempts to exclude bp0 (and bp1).

IVALUE = (**I**)

I=0 — to exclude bp0

I=1 — to exclude bp0 and bp1.

Diraceq : applies Dirac equations to expressions preliminary simplified with the aid of Pulling.

AVALUE = (**i,j,k,l**)

i for spinor tlo, Dirac equation: $\text{tlo } \not{p}_1 = -im_i \text{ tlo}$

j for spinor tro, $\text{tro } \not{p}_2 = im_j \text{ tro}$

k for spinor tre, $\text{tre } \not{p}_3 = -im_k \text{ tre}$

i for spinor tle, $\text{tle } \not{p}_4 = im_l \text{ tle}$

where (**i,j,k,l**) are field indices.

Diracizing : expressions of the form $\hat{q}\Gamma\hat{q}$ and $\gamma_\alpha\Gamma\gamma_\alpha$ are simplified; here $\hat{q} \equiv \gamma \cdot q$, and Γ is a string of up to five γ matrices. The final step consists of setting $\hat{q} \cdot \hat{q} = q^2$ and $\gamma_\alpha\gamma_\alpha = n$, where $n = 4 - \varepsilon$ is the dimension of momentum space.

IVALUE = (I)

I=0 normal use

I=1 a special use in Wff vertices.

DirectProdSumm : performs summation in direct products of γ matrices such as in well known identity

$$\gamma_\mu\gamma_\alpha\gamma_\nu\gamma_6 \otimes \gamma_\nu\gamma_\beta\gamma_\mu\gamma_6 = 4\gamma_\beta\gamma_6 \otimes \gamma_\alpha\gamma_6;$$

this procedure knows 76 identities of such a kind.

AVALUE = (i,j,k,l) , the same arguments as in Diraceq.

DivisionGramDet : realizes various possibilities to use the algebra of Gram determinants to simplify raw expressions.

IVALUE = (I)

I=0 division of det3i (active in all subsequent options)

I=1 division of det4i for O_s, T_s topology, for example T1,T2

I=2 division of det4i for O_s, U_s topology, for example T3,T4

I=3 division of det4i for T_s, U_s topology, for example T5

I=4 division of det4i for U_s, T_s topology, for example T6.

Expansions : expands B_0 and B_0^F functions for small values of some of its arguments.

AVALUE,IVALUE = (FI)

FI field index

ExpansionPhotMassShell : puts an external bosonic momentum in $ffbb$ processes to the corresponding mass shell. For example in the process $ff \rightarrow \gamma B$ for p_γ^2 or p_B^2 its action means

IVALUE,AVALUE = (I,J,mp,pGs,pBs)

I=1, J=1 $pGs = 0, \quad pBs = 0$

I=1, J=2 $pGs = 0, \quad pBs = -mp^2$

I=2, J=1 $pGs = -mp^2, \quad pBs = 0$

I=2, J=2 $pGs = -mp^2, \quad pBs = -mp^2.$

ExtMomentumWl : applies Ward identities for external vector boson momenta, i.e. sets $(p_I)_\mu = 0$ and $(p_I)_\nu = -(p_J)_\nu - (p_K)_\nu$.

AVALUE = (I,mu,J,K,nu)

f2f : realizes the possibility (in particular cases for certain arguments of PV functions) of replacing $B_0 \rightarrow A_0, B_0^F \rightarrow B_0^F, B_0 \rightarrow b_1$ and *vice versa*, if concrete arguments of the PV functions allow such replacements.

AVALUE = (b0,a0) , for example.

FeynmanRules : applies Feynman rules for propagators and vertices, see Section 4.3.

IVALUE = (I)

I=0 for QED part

I=1 for EW and QCD parts.

GammaLeft : all Dirac matrices γ_5 , $\gamma_6 = 1 + \gamma_5$ and $\gamma_7 = 1 - \gamma_5$ are moved to the left and the expression is simplified using identities $(\gamma_5)^2 = 1$, $\gamma_6\gamma_7 = 0$, etc.

GammaRight : the same as in GammaLeft, but all matrices γ_i are moved to the right.

GammaTrace : the traces of products of γ matrices are evaluated in n dimensional space.

Globals : performs global declarations by FORM Tables of particle names, particle masses, electric charges, ghost charges, mass ratios, coupling constants, weak isospins, gauge parameters, combinatorial factors etc.

isoR2Real : realizes the ideology of shifting from the level *in the sense of reduction* p_i to the real 4-momenta p_i , $(p_i)_{input} \rightarrow (p_i)_{output}$ and $(\text{Invariants})_{input} \rightarrow (\text{Invariants})_{output}$, see item **Topologies T5, T6**.

AVALUE = (p1out,p2out,p3out,p4out,Qsout,Tsout,Usout)

Only output values appear in the argument list; the input string is assumed to be p1,p2,p3,p4,Qs,Ts,Us.

m2zero : sets a mass mp to 0 in expressions and in the arguments of all functions.

AVALUE = (mp)

Massshell : This procedure has four arguments, which must be fermionic field indices; a field, whose index is an argument of Massshell, is put on its mass shell. Thus the command `#call Massshell('iu',,,)` sets $p('iu')^2$ equal to $-pm('iu')^2$.

AVALUE = (iu,id,fu,fd) , the same list as in Diraceq.

open : opens a symbol, e.g. substitutes a combination of coupling constants like $vmaen=ven-aen$.

AVALUE = (a)

openall : opens all coupling constants, charges, etc. and then substitutes them.

opensymbol : opens all symbols as openall but only in terms containing symbol 'a'.

AVALUE = (a)

p2D : replaces p_i and p_j by vectors Q and D : $Q = -(p_i + p_j)$ and $D = p_i - p_j$.

AVALUE = (i,j)

p2I : changes a p^2 to an invariant I .

AVALUE = (p,I)

p2m : puts a 4-momentum p to its mass shell, $p^2 = -mp^2$, in the expressions and in the arguments of all functions.

AVALUE = (p,mp)

p2p : changes a p^2 to P^2 and $\hat{p} \rightarrow \hat{P}$ in the string of gamma matrices.

IVALUE,AVALUE = (I,p,P).

I=0 p^2 changes to P^2

I=1 p^2 changes to P^2 and $\hat{p} \rightarrow \hat{P}$

p2Qs : expresses all scalar products $p_i \cdot p_j$ in terms of p_1^2 , p_2^2 and $Q^2 = (p_1 + p_2)^2$ for a three point function with $Q + p_1 + p_2 = 0$.

AVALUE = (p,mp)

PoleSep : separates the PV functions explicitly into their $1/\varepsilon$ pole parts and finite parts A_0^F and B_0^F .

Pulling : is applied to expressions of the form

$$\bar{u}(p_1) (\gamma_\alpha \hat{p}_1 \hat{p}_2 \gamma_\beta \dots) u(p_2)$$

with the result that \hat{p}_1 is placed next to $\bar{u}(p_1)$ and \hat{p}_2 is placed in front of $u(p_2)$, after which the expression is simplified using the Dirac equation by a call to procedure Diraceq.

IVALUE = (I)

I=0 main option, is used in all programs up to ffbb boxes;

eliminates p_4 in ii current and p_2 in jj current

1,2,3,4 is used in ffbb boxes;

eliminates p_1 or p_2 or p_3 or p_4 in ii current. ²

PullingOrder : this procedure orders γ strings containing \hat{p} , γ_μ and γ_ν into $\gamma_\mu \hat{p} \gamma_\nu$ with one of the three factors possibly missing. Thus the surviving expressions are $\gamma_\mu \hat{p} \gamma_\nu$, $\gamma_\mu \hat{p}$, $\gamma_\mu \gamma_\nu$, and $\hat{p} \gamma_\nu$.

AVALUE = (p, μ , ν)

Reduction : it has options l=0, 1: if l=0, then the user can perform a *prereduction*³ “by hand”; if l=1, the *standard prereduction* is done automatically.

After a prereduction is done, the reduction is performed on integrals of the form

$$\int \frac{d^n q \{1, q_\mu, q_\mu q_\nu, \dots\}}{d_0 d_1 d_2 d_3} \quad (60)$$

where $\{1, q_\mu, q_\mu q_\nu, \dots\}$ means one of the expressions: scalar, vector, tensor ⁴ and d_i are given by

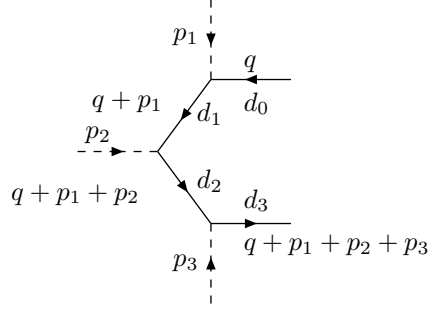
$$\begin{aligned} d_0 &= q^2 + m_1^2, \\ d_1 &= (q + p_1)^2 + m_2^2, \\ d_2 &= (q + p_1 + p_2)^2 + m_3^2, \\ d_3 &= (q + p_1 + p_2 + p_3)^2 + m_4^2. \end{aligned}$$

²See examples of assignment of current labels ii in Figs. 13 and 14.

³The prereduction consists of simplifications, such as the replacement of $q^2/(q^2 + m^2)$ by $1 - m^2/(q^2 + m^2)$.

⁴In the present version of SANC we have tensors of up to the 4th rank and N-point functions for N up to 4.

The N-point function, i.e. a one-loop diagram with N external legs, is defined by the following diagram:



As a result the integrals (60) are replaced by linear combinations of Passarino–Veltman functions $(PV)_{ij} \in \{A_{ij}, B_{ij}, C_{ij}, D_{ij}\}$ where $i = 1, 2, 3$ or 4 for vector, 2nd, 3rd or 4th rank tensor, respectively, and j is a sequential number.

IVALUE = (I)

I=0 works without internal Prereduction

I=1 the standard internal Prereduction is performed

substitute : substitutes an argument “a” (charge, isospin or coupling constant of a particle). For example, to substitute the isospin of the particle ‘typeID’=11 we call `substitute(i3('typeID'))` with the result `i3('typeID')=1/2`.

AVALUE = (a)

Scalarizing : expresses all $(PV)_{ij}$ functions in terms of scalars PV_0 . Option **I=0** acts differently for boxes and N=2,3 point functions; for 4-point functions the masses of the particles with momenta p_1 and p_2 are set equal to zero, for 2,3-point functions Scalarizing is exact in masses. Four digit options are applied only for 4-point functions as explained below. In all cases Scalarizing is exact in masses. Various options have been introduced to save CPU time.

IVALUE = (I)

I=1234 all masses are different

I=1134 masses m_1 and m_2 are equal

I=1133 masses m_1, m_2 and m_3, m_4 are equal

I=1232 masses m_2 and m_4 are equal (for boxes T5, T6)

I=0 masses m_1 and m_2 are equal to zero (for boxes)

The latter option must be used also for self energies and vertices.

Scalarizingdp : Scalarizing of dp_{ij} PV series, see Ref. [1] for definitions of $d \equiv dp$ functions.

IVALUE = (I)

I=0 scalarizing of **dp** series setting masses m_1 and m_2 equal to zero

I=1 scalarizing of **dp** series exact in all masses

ScalarizingProj : acts in *ffbb* boxes of topologies T1, T3, T5 and T6. At first it projects the Input expression into a number of terms according to different structures with corresponding coefficients. Next it starts to apply the procedure *Scalarizing* to each term. The choice of index of *Scalarizing*(I) depends of the type of box topology. Finally, it forms Output expression by summing up all terms.

AVALUE = (k3min,k4min,Topology,NameInput,p,mu,nu,p1,p2,I,NameOutput)
k3min,k4min the indices, defining a cluster, see items **Topologies T1,T3** and **Topologies T5,T6**
Topology number of the topology (1,3,5,6)
NameInput name of input expression
p,mu,nu the same arguments as in **PullingOrder**
p1,p2 fermionic 4-momenta defining basis of structures
I index of procedure *Scalarizing*
NameOutput name of output expression

Scalprod : calculates scalar products for 4-point function with 4-momenta satisfying $p_1 + p_2 + p_3 + p_4 = 0$.

AVALUE = (p)
p scalar products $p_i \cdot p_j$
K scalar products $K_i \cdot K_j$, etc.

Sing : In procedure *Sing*, the dimension n is set equal to $4 - \varepsilon^*$, and then the PV functions, multiplied by ε^* , are analyzed: if a PV function has a pole, then the product $\varepsilon^* \times \text{PV}$ is replaced by its residue, and finally ε^* is set equal to zero.

Symmetrize : symmetrizes Passarino-Veltman functions. Thus B_0 is symmetrized using the symmetry property $B_0(Q^2, m_1, m_2) = B_0(Q^2, m_2, m_1)$.

IVALUE = (I)
I=0 symmetrizes B_0 functions
I=1 symmetrizes B_0 and C_0 functions.

Xi1 : sets all gauge parameters ξ, ξ_A, ξ_Z equal to one. These parameters are present in all intermediate contributions in R_ξ gauge but cancel in gauge invariant physical observables.

4.3 Feynman rules

The **SANC** collection of Feynman rules is based on the Standard Model Lagrangian in R_ξ gauge with three gauge fixing parameters ξ, ξ_A , and ξ_Z [1].

Propagators

Every propagator should be multiplied by a factor of $1/(2\pi)^4 i$.

The propagator of a **fermion** f is a non-commuting function. It is defined by the following **SANC** command:

$$\text{pr}(k,p,ii), \quad \longrightarrow_f$$

where k is the field index, p is the fermionic 4-momentum and ii is the fermionic current label.

The **vector boson** propagator is a commuting function:

$$\text{pr}(k, \mu, \nu, p), \quad \mu \text{ } \text{~~~~~} \nu$$

where k is the field index, μ, ν are the corresponding Lorentz indices and p is the bosonic 4-momentum.

Vertices

In the presently available class of diagrams, *vertices* are of three kinds: boson-fermion-fermion (bff), three-boson (bbb) vertices and four-boson (bbbb) vertices. A *vertex* is a non-commuting function. Every vertex should be multiplied by a factor of $(2\pi)^4 i$.

bff vertices

The **SANC** command for this type of vertex is:

$$\text{vert}(i, l, -j, \alpha, ii),$$

where i, j and l are field indices, α is a Lorentz label and ii is a fermionic current index. The first field index refers to a boson; the other field indices refer to the incoming l and outgoing $-j$ fermion fields.

bbb vertices

The **SANC** command for trilinear vector boson vertices is of the following form:

$$\text{vert}(i, -j, l, \alpha, \mu, \nu, Q, p_1, p_2),$$

where i, j and l are boson field indices, α, μ, ν are Lorentz labels and Q, p_1, p_2 are incoming momenta such that $Q + p_1 + p_2 = 0$. Significant is that the triplets of arguments, $\{i, -j, l\}$, $\{\alpha, \mu, \nu\}$ and $\{Q, p_1, p_2\}$ are written in the same order according to the rule: “*from ingoing neutral to ingoing negative charge flow*”, where the positive charge flow is shown by the arrows in the diagram.

In the vertex diagrams involving a Higgs boson or scalar unphysical fields (Higgs-Kibble ghosts), the Lorentz indices μ are shown in brackets since they are *dummy* or *silent* indices, kept in the **vert** command for formal reasons, whereas these vertices do not depend on μ .

In the book [1] all tri-linear bosonic vertices together with their Feynman rules, involving Higgs bosons, scalar unphysical fields ϕ^0 and ϕ^\pm and Faddeev-Popov ghosts are shown. Many of these diagrams carry silent (or dummy) Lorentz indices as discussed above in connection with *bff* vertices, and also dummy 4-momenta.

bbbb vertices

The **SANC** command to define this class of vertices is (see the generic diagram)

$$\text{vert}(i, j, k, l, \alpha, \beta, \mu, \nu),$$

where i, j, k, l are field indices and α, β, μ, ν are corresponding Lorentz indices.

In the book [1] all quadri-linear bosonic vertices together with their Feynman rules are presented.

5 Processes, available in SANC v.1.00

In this section we briefly discuss the available in QED and EW branches processes. In this paper we do not discuss processes of QCD branch which are scarce.

The Fig. 18 shows the fully open menu for “Processes” in the QED branch of **SANC** whose structure we briefly describe. The Figures 19 show all available 3-leg and 4-leg EW processes. We will not describe them in this part of the description since after explaining the QED branch, they may be easily interpreted. Moreover, the QED branch has mostly a pedagogical purpose. This is why it is worth devoting some time to it already in this first part mostly dealing with Precomputation. However, we will not describe here the structure of corresponding modules, leaving this for a second part of the **SANC** description. QED processes are presented by three classes: 1) a heavy photon decay; 2) e^+e^- annihilation into a lepton pair (including Bhabha scattering); 3) Compton-like processes, i.e. $e^+e^- \rightarrow \gamma\gamma$ or some other cross channel. Note that by our convention QED contains massless photons and three generations of leptons. We consider, nevertheless, the decay of a heavy photons for pedagogical reasons.

When we arrive via a menu sequence, *e.g.* **QED** \rightarrow **Processes** \rightarrow **A** \rightarrow **II Decay**, we normally see three modules **FF**, **HA** and **BR**. Modules **FF** compute the scalar form factors of a given process. As was already stressed, they are channel independent, modulo a crossing transformation. Then a FORTRAN code to compute them can be automatically generated as described in Section 6. Modules **HA** compute channel dependent HAs. The channel is evident for examples 1) and 2); for example 3) we have for the time being HAs for the annihilation channel $e^+e^- \rightarrow \gamma\gamma$ and for the inverse channel $\gamma\gamma \rightarrow e^+e^-$.

Both in QED and EW branches, modules **BR** compute analytically the contributions due to accompanying Bremsstrahlung. In this connection, present implementation of Bremsstrahlung into **SANC** is not homogeneous. As a rule, for all $1 \rightarrow 2$ decays we have both Soft and Hard photon contributions. If only neutral particles are involved, for example $Z \rightarrow \nu\nu$, the module **BR** is not present in the tree. There is one exception: for $Z \rightarrow W^+W^-$ decay we have only one module **FF**, since it is unphysical and we implemented **FF** for future use as a building block for more complicated processes. As a rule, for $4f$ processes we also have both Soft and Hard photon Bremsstrahlung with exception of Bhabha process where we have only Soft contribution. For $CC\ 2f_1 \rightarrow 2f$ processes where we have realized quite involved calculations of Hard Bremsstrahlung with a possibility to impose simple cuts, see also [29]. For the tree body decays $t \rightarrow b\nu$ we have implemented both Soft and Hard contributions. For $2f2b$ processes we had so far no **BR** and no **s2n** calculations.

This work is being started in version 1.10, where we have implemented **FF** and **HA** modules for three more $ffbb$ processes: $f_1\bar{f}_1 \rightarrow ZZ$, $f_1\bar{f}_1 \rightarrow ZH$ and $H \rightarrow f_1\bar{f}_1Z$. We recall, that f_1 stands for a massless fermion (its mass is retained only in the arguments of logs, if necessary). For the decay channel $H \rightarrow f_1\bar{f}_1Z$ and annihilation process $f_1\bar{f}_1 \rightarrow ZH$ we have implemented (**BR**) modules and **s2n** calculations, see also [30] which contains an extensive presentation of numerical results.

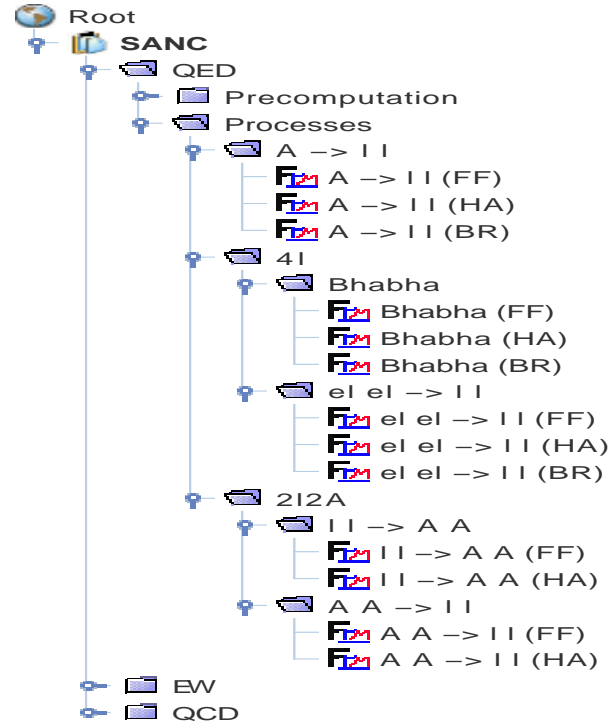


Figure 18: Available processes in QED part.

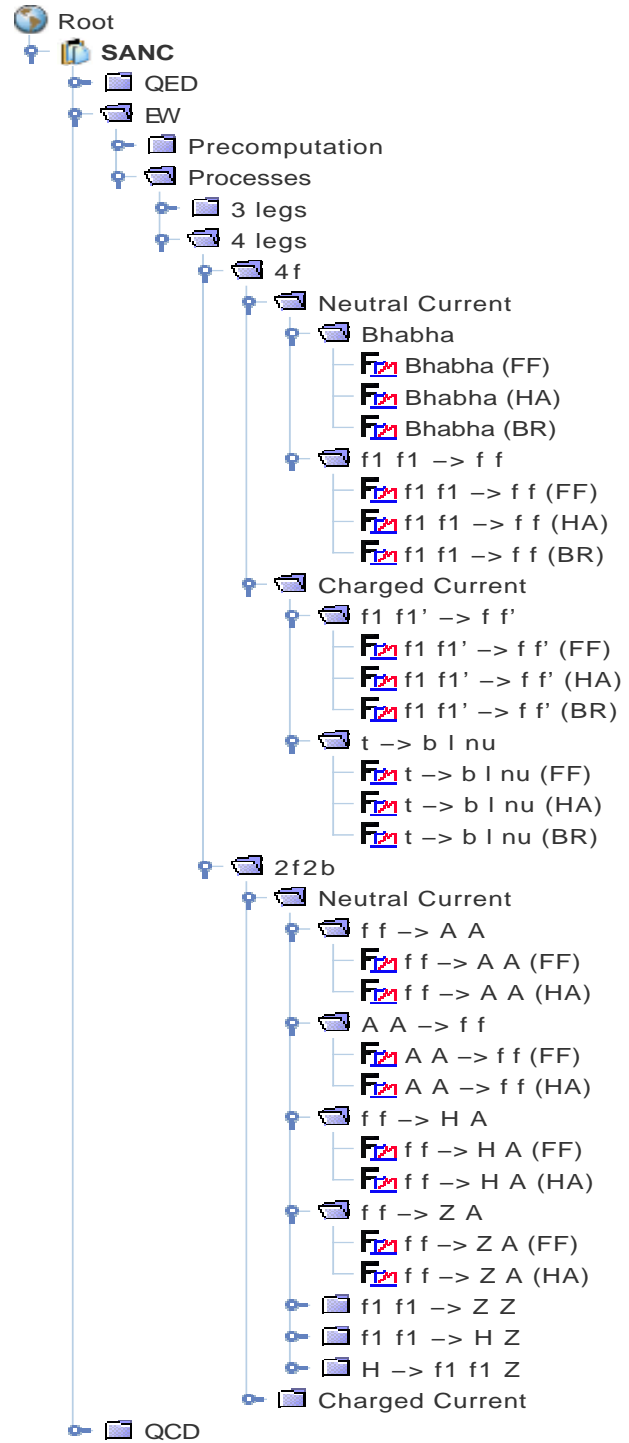
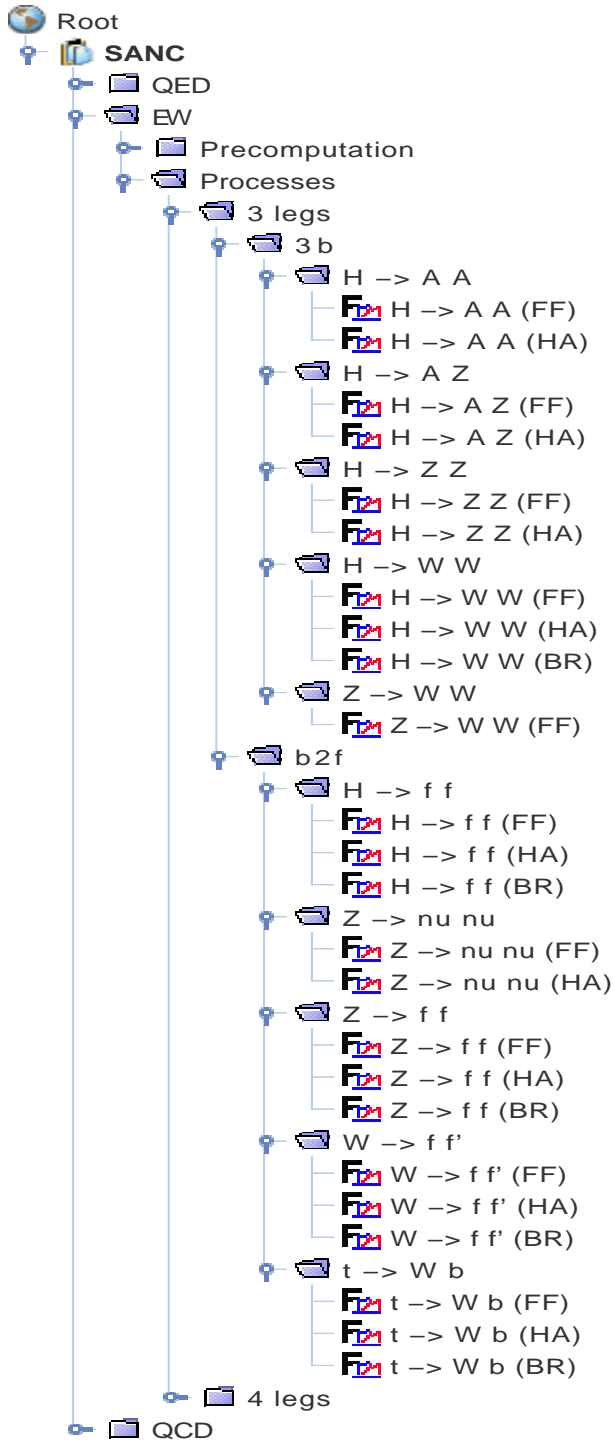


Figure 19: Available processes in EW part.

6 User Guide

6.1 Getting started

6.1.1 SANC installation

To work with SANC, one must install a SANC client on ones computer. The SANC client can be downloaded from the SANC project homepage <http://sanc.jinr.ru> or <http://pcphsanc.cern.ch>. On the homepage select **Download**, then download the client appropriate for your operational system (Linux, Windows), save it to your home directory and follow the instructions.⁵

In Linux, opening the *.tgz file creates the directory `/home/<user>/sanc_installer`. Change to that directory, read the **Readme** and execute `install.sh`. SANC is then installed in `/home/<user>/sanc_1.00.00`. To start a SANC session, go to directory `/home/<user>/sanc_1.00.00/bin` and execute `sanc`.

In Windows, start `sanc_installer.exe` program and follow the instructions, restart computer. To start a SANC session, click SANC client icon.

6.1.2 SANC windows

At the beginning of a client session the main SANC window opens, see Fig. 20,⁶ with several **toolbars** and **windows** or **fields**:

- on top is the **Menu bar** with menus *File*, *Edit*, *Build*, *Applications* and *View*;
 - underneath is a row of three **Toolbars**: **File**, **Edit** and **Build**
 - underneath that on the left is the **SANC tree** field, and to the right of it the **Editors List** window;
 - underneath is the **Output** window and underneath that is the **Console**;
 - below, at the bottom, lies the **Status** bar.
- Other fields do arise in the course of the work.

The five menus have the options shown in Table 1. Menus with \rightarrow have further extensions. For example, *Toolbars* has four options; they duplicate the *File*, *Edit* and *Build* toolbars, which are activated by default, and a latent option *Memory*. When the latter option is activated, two numbers are displayed: the first one is the current usage of the Java Virtual Machine (JVM) memory, and the second one is the total size of the JVM memory. All options can be unchecked in menu *View* \rightarrow *Toolbars* \rightarrow .

6.1.3 Login procedure

- To log in, click the **Login** icon (the first icon of the File toolbar). The Login panel opens with a choice of SANC servers: *local*, *sanc.jinr.ru* and *pcphsanc.cern.ch*; choose one of the latter ones (the *local* server is for PCs which have the server itself installed), then enter the login name *guest* and password *guest*.
- Click the **Open Project** icon (the second icon of the File toolbar). This opens the **Open Project** panel. There are two projects: **Lessons** and **SANC**. Select project **SANC** and press **OK**; then the **SANC tree** appears in the **SANC tree** field.

6.1.4 The SANC tree

The **SANC tree** has three options: **QED**, **EW** and **QCD**. Selection of one of these opens the next level of options: **Precomputation** and **Processes**.

⁵To install and run SANC client one should have the Java Runtime Environment (JRE) at least version 5.0 Update 5 installed, see section **Minimum System Requirements** of the **Download** page at the SANC project homepage.

⁶In the figure the windows are shown after several of the steps described below.

Table 1: The **SANC** Menus and their options.

<i>File</i>	<i>Edit</i>	<i>Build</i>	<i>Applications</i>	<i>View</i>
<i>Login ...</i>	<i>Undo</i>	<i>Compile</i>	<i>Editor Form</i>	<i>Toolbars →</i>
<i>Open Project ...</i>	<i>Redo</i>	<i>Run S2N</i>	<i>Numeric Form</i>	<i>Projects</i>
<i>Mount Filesystem →</i>	<i>Cut</i>		<i>Graphics Form</i>	<i>Editors List</i>
<i>Unmount Filesystem</i>	<i>Copy</i>			<i>Processes Table</i>
<i>Save</i>	<i>Paste</i>			<i>Console</i>
<i>Save All</i>	<i>Find</i>			<i>Output</i>
<i>Print ... →</i>	<i>Replace</i>			<i>Status Bar</i>
<i>Exit</i>	<i>Settings</i>			<i>ProgressBar</i>
				<i>Full Screen</i>
				<i>Look And Feel →</i>
				<i>Suggestions</i>

Here we describe the sequence of steps for option **EW > Processes**. The use of the **Precomputation** branch was described to an extent in Section 3.

The available processes are subdivided into **3legs** and **4legs**. The two branches of **3legs** are **3b** and **b2f** decays, and those of **4legs** are **4f** and **2f2b** processes; here **b** and **f** denote any *boson* and *fermion*, respectively. For each of the latter two there is a branch for **Neutral Current** and a branch for **Charged Current** processes. The next branching is into the available processes of that class.

6.1.5 Naming conventions

In **SANC** we use naming conventions for fields (or particles) shown in Table 2 where *N* is the field index, and in the columns headed “name” we show the names used internally in **SANC**. All associated parameter symbols are derived from these names. Thus the mass, charge and weak isospin of the electron are denoted **m_{e1}**, **q_{e1}** and **i_{3e1}**, respectively, also the vector and axial vector coupling constants (**v_{e1}**, **a_{e1}**) and their sum (**vp_ae1**) and difference (**vm_ae1**).

Table 2: List of fields.

bosons			fermions									QCD		
			1st generation			2nd generation			3rd generation					
<i>N</i>	field	name	<i>N</i>	field	name	<i>N</i>	field	name	<i>N</i>	field	name	<i>N</i>	field	name
1	A	gm	11	ν_e	en	15	ν_μ	mn	19	ν_τ	tn	23	g	gn
2	Z	z	12	e^-	el	16	μ^-	mo	20	τ^-	ta	24	Y_g	-
± 3	W^\pm	w	13	u	up	17	c	ch	21	t	tp			
4	H	h	14	d	dn	18	s	st	22	b	bt			
5	ϕ^0	-												
± 6	ϕ^\pm	-												
7	X^+	-												
8	X^-	-												
9	Y_z	-												
10	Y_A	-												

6.2 Benchmark case 1: $b \rightarrow ff$ decays

6.2.1 Semianalytical calculation

Consider the $Z \rightarrow b\bar{b}$ decay. First we open the relevant branch of the **SANC** tree:

$$\mathbf{EW} \rightarrow \mathbf{Processes} \rightarrow \mathbf{b2f} \rightarrow \mathbf{Z} \rightarrow \mathbf{ff}$$

There are three FORM programs: (**FF**) *Form Factor*, (**HA**) *Helicity Amplitudes*, and (**BR**) *Bremsstrahlung*.

Select (**FF**) by a click with the right mouse button, this also pulls down a menu. On the menu left-click on **Open**. A **Source Editor** window opens with three tags: **Form Editor**, **Fortran Editor**, and **Monte Carlo Editor**. The first of these is activated by default and the FORM source code is displayed in the field.

The particle indices can be seen in the **Console** field; by default they are: **typeB** = 2 (Z boson), **typeU** = 22 and **typeD** = 22 (b quarks). To change the final state fermions, their particle numbers can be changed by editing them in the **Console** field and pressing **Enter**.⁷

After choosing the process, open the **Numeric Form** panel from the *Application* menu. In this panel the particle masses and other relevant information are displayed.

Next the FORM code is compiled by clicking on the **Compile** button — the first icon in the **Build** toolbar (or by pressing the **F7** function key). After compilation the FORM *log file* is shown in the **Output** field.

Clicking on the **Run S2N** button generates the FORTRAN code; the FORTRAN code can be seen in the **Output** field.

Repeat the sequence of steps for (**HA**) and (**BR**).

The progress of work can be monitored by activating the **Processes Table** (see Table 1).

The entire **Output** field is arranged in sheets with tags; for inspection any sheet can be brought to the foreground by clicking on its tag.

Once the three FORM codes (**FF**), (**HA**) and (**BR**) have been compiled and tranfered to the FORTRAN codes one can get the numeric results by the following sequence of operations:

- (i) open the *FORTTRAN editor* sheet of the **Editors List** (belonging to the (**FF**) FORM code),
- (ii) open the **Numeric Form** panel from the **Applications** menu,
- (iii) press the **Rehash** button at the bottom of the **Numeric Form** panel, then the **Compile** button.

The answer appears in the **Output** field. It consists of a list of **Input parameters** and a set of results: $\Gamma(\text{born})$, the total width [TotalWidth] in Born approximation, $\Gamma(\text{born+virt+soft})$ and the total width, $\Gamma(\text{born+virt+soft+hard})$. Also shown is the parameter ω , set to 10^{-10} GeV by default. This parameter defines the separation between soft and hard radiation. It can be modified in the corresponding box of the **Numeric Form** panel. Rerunning the program after changing the value of ω (using the sequence **Rehash** > **Compile**) gives a result that differs only in the value of $\Gamma(\text{born+virt+soft})$. The born+virt+soft width is sensitive to parameter ω and can become unphysical (negative) for very small values of ω . Increasing ω and rerunning gives positive values.

⁷This need be done only once for a particular choice; to repeat, put the cursor at the end of the **Console** field, press the down-arrow key, select the required line of particle numbers using the up- and down-arrow keys and confirm by pressing **Enter**.

Table 3: Benchmark Results for $\Gamma(Z \rightarrow b\bar{b})$ decay

	Γ_{Born}	$\Gamma_{Born+virt+soft}$	Γ_{Total}
SA	0.356948	0.336732	0.360224
MC 100 k			0.360229 ± 0.000721

6.2.2 Monte Carlo calculation

The user can also carry out a Monte Carlo calculation generating various histograms: **Photon Energy**, **Fermion Energy**, **Photon-Fermion Angular** and **Fermion-antiFermion Angular**. To do this one must bring the Monte Carlo sheet of the **Numeric Form** to the foreground, check the boxes of the required histograms, then bring the MC sheet of the **Editors List** to the foreground and rerun the program by clicking the **Compile** button. After a while the **Histogram Form** is displayed. This form has a menu bar; menu *Option* allows display of the histogram statistics. On the Monte Carlo sheet one can also select the random number generator,⁸ modify the number of MC events and the range of real photon energies $k_{0\min}$ and $k_{0\max}$, where $k_{0\min} = \omega$ and $k_{0\max}$ can be used as an experimental cut. The **Rehash** button must be pressed after each change in the **Numeric Form** before clicking on the **Compile** button.

The results for the decay rates (in GeV) of the semianalytical calculation and of the Monte Carlo calculation for 100 000 events are summarised in Table 3. The numerical values are truncated to 6 significant figures.

6.3 Benchmark case 2: the process $2f \rightarrow 2f$

Consider the $4f$ **CC** process $f_1\bar{f}'_1 \rightarrow f\bar{f}'$. Implemented are the processes $u\bar{d} \rightarrow \ell^+\nu_\ell$, its charge conjugate and the decay $t \rightarrow b\ell^+\nu_\ell$. For each process there are three FORM programs: (**FF**) *Form Factor*, (**HA**) *Helicity Amplitudes*, and (**BR**) *Bremsstrahlung*. Each of these in turn is opened, compiled and run as above in Section 6.2.

For process $u\bar{d} \rightarrow e^+\nu_e$ we have in the **Console** window the particle indices shown in Table 4. These

Table 4: Assignment of particle numbers for process $u\bar{d} \rightarrow e^+\nu_e$

typeIU = 14	initial Up-type antiparticle (\bar{d} quark)
typeID = 13	initial Down-type particle (u quark)
typeFU = 12	final Up-type antiparticle (positron)
typeFD = 11	final Down-type particle (neutrino)

can be changed to typeIU = 13, typeID = 14, typeFU = 11 and typeFD = 12 for process $\bar{u}d \rightarrow e^-\bar{\nu}_e$ by editing the particle numbers as explained above⁹.

Next bring the *Fortran Editor* sheet of the **Editors List** and the **Numeric Form** panel to the foreground. Shown on the **Numeric Parameter** sheet are the particle masses in GeV/c^2 and the CMS energy in GeV, also the cosine of the CMS angle between the incident and outgoing particle momenta.

Click on the **Rehash** button at the bottom of the **Numeric Form** panel: the main module of FORTRAN code appears in the *Fortran Editor* sheet of the **Editors List**. Then click on **Compile**. The

⁸Three random number generators provided are: Ranlux, Ranmar and Mersenne Twister.

⁹See Fig. 13a) for definitions of particle types typeXX.

final answer appears in the **Output** field. It consists of the parameters used (α , G_F , particle masses, the 't Hooft scale μ and the Mandelstam variables), and the resulting differential cross sections $d\sigma/d\cos\theta$ in picobarns in the **Born** approximation and **Born+one-loop**. The results for the default parameters and for several scattering angles are summarised in Table 5. The numerical values are truncated to 6 figures.

Table 5: CMS differential cross sections in pb for $u\bar{d} \rightarrow e^+\nu_e$

$\cos\theta$		\sqrt{s} GeV		
		40	80	120
-0.9	Born	3.58202	10818.4	12.0561
	Born + one-loop	3.53427	9990.97	28.1226
-0.5	Born	2.23256	6742.78	7.51423
	Born + one-loop	2.18961	6226.00	12.8563
0.0	Born	0.99225	2996.79	3.33966
	Born + one-loop	0.97192	2769.11	5.12160
0.5	Born	0.24806	749.198	0.83491
	Born + one-loop	0.24453	695.224	1.47999
0.9	Born	0.00992	29.9679	0.03339
	Born + one-loop	0.01072	30.2878	0.09277

Here the one-loop corrections are purely weak and QED corrections comprise one-loop virtual QED corrections and soft and hard radiations.

The **Born+one-loop** cross section is insensitive to the 't Hooft scale parameter μ which cancels between one-loop electroweak and the QED part of virtual corrections.

Input parameters can be changed by editing the appropriate field of the **Numeric Form** panel and pressing the **Rehash** button. Again the **Rehash** button must be pressed before pressing **Compile**.¹⁰

In the NC sector there are many more processes. Here f_1 is a *massless* fermion of the *first generation*¹¹ or *any* neutrino, and f is *any* fermion. All procedures described above for the CC processes apply also in this case.

Monte Carlo calculations are not yet implemented for $2 \rightarrow 2$ processes.

Acknowledgments

The authors are very much indebted to G. Passarino for critical reading of the manuscript and useful comments. We are grateful to S. Jadach, W. Placzek, F. Tkachov, B. Ward, and Z. Was for numerous discussions. We thank V. Kolesnikov and E. Uglov for managing and supporting the SANC computer system.

¹⁰To produce whole Table 5 one can set flag `tbprint = 1` in the *Fortran Editors* sheet. After editing the code one has not need press the **Rehash** button, but just **Compile**.

¹¹The masses of first generation fermions are retained only in logs to regulate collinear singularities.

References

- [1] D. Bardin and G. Passarino, *The standard model in the making: Precision study of the electroweak interactions*. Clarendon, 1999. Oxford, UK.
- [2] D. Bardin, G. Passarino, L. Kalinovskaya, P. Christova, A. Andonov, S. Bondarenko, and G. Nanava, *Project CalcPHEP: Calculus for precision high energy physics*, Proceedings of the International Workshop on Computer Algebra and its Application to Physics, CAAP-2001, Dubna 2001. Edited by V.P. Gerdt.
- [3] D. Bardin *et al.*, *Comput. Phys. Commun.* **133** (2001) 229–395.
- [4] A. Arbuzov *et al.*, *Comput. Phys. Commun.* **94** (1996) 128–184.
- [5] D. Bardin, J. Blumlein, P. Christova, and L. Kalinovskaya, *Nucl. Phys.* **B506** (1997) 295–328.
- [6] D. Bardin and L. Kalinovskaya, *QED corrections for polarized elastic μe scattering*, hep-ph/9712310.
- [7] J. A. M. Vermaseren, *New features of FORM*, math-ph/0010025.
- [8] D. Bardin, P. Christova, L. Kalinovskaya, and G. Passarino, *Eur. Phys. J.* **C22** (2001) 99–104.
- [9] A. Andonov *et al.*, *Phys. Part. Nucl.* **34** (2003) 577–618.
- [10] A. Arbuzov, D. Bardin, and L. Kalinovskaya, *Radiative corrections to neutrino deep inelastic scattering revisited*, *JHEP* **06** (2005) 078. hep-ph/0407203.
- [11] A. Andonov *et al.*, *Nucl. Instrum. Meth.* **A502** (2003) 576–577.
- [12] L. V. Kalinovskaya, *Nucl. Instrum. Meth.* **A502** (2003) 581–582.
- [13] P. Christova, *Nucl. Instrum. Meth.* **A502** (2003) 578–580.
- [14] G. Nanava, *Nucl. Instrum. Meth.* **A502** (2003) 583–585.
- [15] A. Andonov *et al.*, *Project SANC (former CalcPHEP): Support of analytic and numeric calculations for experiments at colliders*, Proceedings of 31st International Conference on High Energy Physics (ICHEP 2002), Amsterdam, The Netherlands, 24–31 Jul 2002. Amsterdam 2002, ICHEP pp.825–827, hep-ph/0209297.
- [16] D. Bardin, P. Christova, and L. Kalinovskaya, *Nucl. Phys. Proc. Suppl.* **116** (2003) 48–52.
- [17] D. Bardin and L. Kalinovskaya, *Present Status of CalcPHEP Project and Update of one-loop corrections for $e^+e^- \rightarrow f\bar{f}$, first run of CalcPHEP system*, 2002, ECFA Study Workshop, Saint-Malo, France.
- [18] D. Bardin and L. Kalinovskaya, *Project SANC: Ideas and Realization and SANC: $2 \rightarrow 2$ Processes*, 2003, CERN Workshop on Monte Carlo generators for LHC, Geneva.
- [19] D. Bardin, L. Kalinovskaya, and A. Arbuzov, *Present Status of the Project SANC and SANC: $2 \rightarrow 2$ Processes and SANC and Deep Inelastic Neutrino Scattering*, 2003, ECFA Study Workshop, Montpellier, France.
- [20] A. Arbuzov, D. Bardin, and L. Kalinovskaya, *Electroweak radiative corrections to neutrino DIS*, talk presented at Linear Collider Workshop in Paris, 19–23 April 2004, to appear in Proceedings.

- [21] R. Vega and J. Wudka, *Phys. Rev.* **D53** (1996) 5286–5292.
- [22] R. Kleiss and W. J. Stirling, *Nucl. Phys.* **B262** (1985) 235–262.
- [23] T. Hahn, *Comput. Phys. Commun.* **140** (2001) 418–4570.
- [24] J. Fleischer *et al.*, *One-loop corrections to the process $e^+e^- \rightarrow t\bar{t}$ including hard bremsstrahlung*, hep-ph/0203220.
- [25] J. Fleischer *et al.*, *Complete electroweak one-loop radiative corrections to top-pair production at TESLA – a comparison*, LC-TH-2002-002, hep-ph/0202109.
- [26] A. Andonov, S. Jadach, G. Nanava, and Z. Was, *Acta Phys. Polon.* **B34** (2003) 2665–2672.
- [27] G. Nanava and Z. Was, *Acta Phys. Polon.* **B34** (2003) 4561–4570.
- [28] A. Andonov *et al.* *A second part of the SANC description*, in preparation.
- [29] A. Arbuzov *et al.*, *One-loop corrections to the Drell–Yan in SANC (I). The Charged Current case*. Jun 2005. 11pp. hep-ph/0506110.
- [30] D. Bardin *et al.*, *SANCnews: Sector $f\bar{f}b\bar{b}$* . Jun 2005. 16pp. hep-ph/0506120.